Sedimentary Geology 442 (2022) 106291

Contents lists available at ScienceDirect

Sedimentary Geology

journal homepage: www.elsevier.com/locate/sedgeo

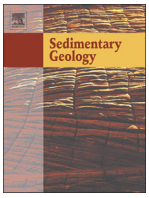

Facies model, cementation and sedimentary evolution of a 20th-century beach and beachrock: The Gorrondatxe wave and tidal coastal system (NE Spain)

José F. García-Hidalgo [a,*], Javier Elorza [b]

[a] Departamento de Geología, Geografía y Medio Ambiente, Universidad de Alcalá, 28871 Alcalá de Henares, Spain
[b] Departamento de Geología, Universidad del País Vasco, Apartado 644, 48080 Bilbao, Spain

ARTICLE INFO

Article history:
Received 24 August 2022
Received in revised form 3 November 2022
Accepted 4 November 2022
Available online 09 November 2022

Editor: Dr. Massimo Moretti

Keywords:
Facies model
Cementation
Sedimentary evolution
Beach
Beachrock
Spain

ABSTRACT

Lithology, bedding, and sedimentary structures of the Gorrondatxe coastal and beach system show an upper shoreface around the low-water level and containing the coarsest grain sizes; a foreshore in the main intertidal zone, which is mainly composed of sands with minor gravels and a distinctive low-angle, seaward-dipping, planar-parallel lamination; and a backshore zone with a mixture of marine-derived sands (washover) and non-marine sands and muds (aeolian, subaerial ponds) above the high-tide water level. The facies model shows a wave-dominated, mesotidal, composite beach with a fining-upwards and aggradational trend. Over the 20th century, a beachrock developed in this area as a result of heavy-industry waste dumping (steel industry) off the coast, which later became attached to the coast. There are a variety of cements and degrees of lithification in the beachrock, suggesting that the beachrock-related processes, although coetaneous, were not similar in all these zones and that different cements developed at the same time. Sand cementation can be used to recognize such facies in the stratigraphic record or in well cores, when other kinds of data are not available. The upper shoreface sandstones are hard and well-cemented, with a whitish circumgranular aragonite cement and good intergranular porosity; the foreshore sands are medium-hard, with a brown, irregular, aragonite needle cement, which shows higher intergranular porosity; finally, the backshore sands are only lightly cemented, with a brown aragonite and rhombohedral calcite cement, with the highest intergranular porosity. SEM images show the presence of *Coccus*-type bacteria in all the different facies and zones; these are the best proof of metabolic activity, probably of ureolytic bacteria, in the origin of all these cements. Over the course of the 20th century, Gorrondatxe evolved from a formerly dissipative, ridge and runnel beach to an active, aggrading and prograding, reflective beach, and finally to an inactive beach prone to erosion. The change to a reflective profile and the cementation of the beachrock indicate that anthropic offshore inputs were rapidly recycled into the beachface. Another major change occurred when waste discharges ended, and the former sediments and beachrock started to be eroded to their current state.

© 2022 The Author(s). Published by Elsevier B.V. This is an open access article under the CC BY-NC-ND license (http://creativecommons.org/licenses/by-nc-nd/4.0/).

1. Introduction

Beachrocks are consolidated coastal beach deposits, which become bonded together relatively fast due to the precipitation of calcite and/or aragonite cements (Moore and Billings, 1971; Hanor, 1978; Binkley et al., 1980; Gischler and Lomando, 1997; Vousdoukas et al., 2007; Friedman, 2011; and references herein). Usually, the overall importance of beachrocks is based upon three main points: their significance as former sea-level indicators (Hopley, 1986; Mauz et al., 2015); their presence as evidence for the processes of rapid shallow carbonate cementation on beaches (Taylor and Illing, 1969; Wiles et al., 2018); and the influence they exert and the changes they undergo related to their origin and development in coastal areas (Vousdoukas et al., 2007).

Many current beachrock studies, however, are almost exclusively petrographic and do not consider the facies variations that may occur within beachrocks, ignoring important elements of the sedimentary environments. In this sense, because of their rapid cementation, another important point in the study of beachrocks is precisely the conservation of beach sedimentary structures and textures during their lithification. Then, beachrock deposits are sedimentary features, present in modern coastal systems, that may act as a bridge between them and the past stratigraphic record. Distinguishing between the different sandy facies in these systems, deposited in the different beach zones, can be locally difficult for facies model development. Sedimentary structures are the

* Corresponding author.
E-mail addresses: jose.garciahidalgo@uah.es (J.F. García-Hidalgo), josejavier.elorza@ehu.eus (J. Elorza).

https://doi.org/10.1016/j.sedgeo.2022.106291
0037-0738/© 2022 The Author(s). Published by Elsevier B.V. This is an open access article under the CC BY-NC-ND license (http://creativecommons.org/licenses/by-nc-nd/4.0/).

main criteria for facies differentiation, but in zones where different sandy facies interfinger, a precise interpretation may be challenging since many sands are parallel-laminated. The presence of a beachrock and the different processes that give rise to its cements offer a series of evidence on the sedimentary environment at the time of cementation (Vousdoukas et al., 2007) and can be useful for the differentiation of facies in these beach zones. Regardless of the diverse sedimentary structures preserved in beachrocks and their potential for detailed sedimentary interpretations (Kelly et al., 2014), comprehensive studies linking a detailed lithofacies analysis of sedimentary environments and the kind of beachrock cementation of these environments are scarce from the scientific literature.

On the other hand, several points regarding the origin and properties of beachrock are still subject to debate and remain partially unresolved, mainly the processes controlling the cementation. Thus, the CO_2 degassing of shallow groundwater (Hanor, 1978), evaporation (Taylor and Illing, 1969; Moore and Billings, 1971), the mixing of marine and meteoric waters (Schmalz, 1971; Moore, 1973), and the direct or indirect activity of organisms (Webb et al., 1999; Neumeier, 1998, 1999) have all been suggested as the most important processes responsible for cement precipitation.

In this context, the recent development of beachrock on the Gorrondatxe wave and tidal coastal system, located on the north coast of Spain, offers a superb opportunity to study several of the above-mentioned issues and thereby attain a more precise understanding of coastal systems and on the origin of beachrock cementation. One of the main features of the studied beachrock and beach is that they are mainly composed of a mixture of anthropic, man-made materials and coastal sediments. Human activities and natural processes, as discussed below, were the main factors in the deposition and the concentration of the man-made gravels and sands at the beach, and all these scoria clasts can be considered Anthropocene technofossils in the sense of Zalasiewicz et al. (2014).

The main objectives of the study are: (a) to document and evaluate the sedimentary structures, textures, and composition of the facies and the facies relationships in the Gorrondatxe beachrock and the related, post-beachrock, surface sediments; (b) to establish and distinguish the depositional environments of various beachrock outcrops within the tidal zone, and their modern counterparts along the beach. Particularly, this study tries to establish a facies model based on these sedimentological and stratigraphical relationships; (c) to analyse and compare the beachrock with modern sediments that have been influenced by the addition of industrial by-products; (d) to determine the origin and cementation mechanisms of the beachrock sediments; and (e) to elucidate the 20th-century development of the beach, focusing on a comparison both between Gorrondatxe and other nearby, present-day beaches and the beach configuration through time, before and after the anthropic materials were deposited off the beach in the early 20th-century.

2. Study Area

The Gorrondatxe coastal system is a north-facing beach and backshore area located on the coast of the Basque Country (NW of Bilbao, Spain). Gorrondatxe lies within an embayment located along a cliff and rocky coastline and is bounded by two large headland promontories composed of Paleogene turbiditic limestone and marl alternations (Fig. 1). It is exposed to brief, North Atlantic storm periods and is therefore subject to high-energy waves, interspersed between often long periods of calm wave conditions mainly in summer. Waves thus reach this section of the coastline mostly from the north-northwesterly quadrants, with clear oceanographic seasonality. Climate records throughout the 20th century in the nearby Bilbao town (Fig. 1) show a return to conditions of greater climatic regularity, comparing to 19th century; with relatively homogeneous temperatures (12.1 °C; annual average temperature) and precipitations (1197 mm; annual accumulated average precipitation), lacking drier phases or drought periods, although there is a large gap in precipitation data between 1920 and 1947.

Gorrondatxe can be considered an unbarred, reflective beach, with a clear predominance of wave processes. The reflective part of the beach is mainly flat and shows a seaward dip of up to 7°; beach cusps develop temporarily during storms, related to strong wave action. The transverse profile of the beach is flat-concave-flat in shape. Based on nearshore wave processes, the beach can be subdivided into three well-defined sedimentary beach zones, related to hydrodynamic zones: a) a flat backshore with a storm berm, with the development of ponds and aeolian sediments (Fig. 1); b) a concave, steep and reflective upper foreshore in the swash-backwash zone; and c) a sharp break point (plunge step) with a low, flat terrace located in the upper shoreface, dominated by shoaling, surf and breaker waves. The width of the foreshore ranges from 40 to 60 m with berm crest elevations of 30 (east)-120 cm (west) above the high-tide water level. The width of the backshore ranges from 20 (west) to 150 m (east). The predominant process in the beach environment is wave swash and backwash, which runs up the foreshore and occasionally overtops the berm during high tides and storms.

An outstanding feature of this coast is the development and dismantling of a beachrock, probably within the last 120 years, on the Gorrondatxe and Arrigunaga reflective beaches, and the Tunelboka, Punta Galea coastal abrasion platform (Fig. 1). It is noteworthy that beachrocks developed in this particular part of the coast, but that no other beachrocks have formed in other, more distant beaches along the Basque coast, either to the east or the west. The beachrock is made up of a mixture of anthropic materials and coastal sediments of significant volume (>6 m thick), and since there is no other beachrock further along the coast, its origin and development are clearly related to the presence of slag deposits deposited in nearby open-marine areas, which were later transported to the shore. Slag, which is a by-product of the reduction of iron ore to iron and steel, was disposed of in nearby open-marine areas from 1895 to the mid-1960s. Since that time, many fragments have reached all the beaches east of Bilbao. Steel industry wastes consist mainly of slag but also contain casting bricks, foundry sand, wood, boat lines, ship ropes, tyres, various kinds of plastic (including nylon) and other refractory material (Astibia, 2012).

These circumstances have attracted numerous groups of researchers, who have studied the phenomenon with different objectives and points of view.

Knox (1973) was the first author to recognize the presence of a beachrock in the Punta Galea-Tunelboka area, considering it to be of very recent age and composed of volcanic materials and refractory bricks, all cemented both by aragonite and by diffuse forms of haematite as an alteration product. His initial confusion regarding the presence of volcanic materials is rectified in a note at the end of the paper, in which he points out that the previously mentioned volcanic rocks were in fact remains of foundry slag from blast furnaces.

Following this initial paper, several further papers dealt with the origin, composition, distribution, and volume of industrial discharges. Moreover, the presence of aragonite was confirmed as the main cementation phase of the beachrock, as was the extreme readiness of its formation, and the role of anthropic intervention in its partial removal in several areas (Aizpiri, 1983; García-Garmilla, 1990; Astibia, 2012; Pujalte et al., 2015). Geomorphological changes due to the subsequent (1995–1999) regeneration of the Arrigunaga beach have also been addressed (Elorza, 2021). Recently, greater attention has been paid to determining the general chemical compositions of the beachrock and its cements, and in particular the ferruginous cements related to the weathering of the slags, using conventional analytical techniques and Raman spectroscopy in combination with SEM-EDX (Iturregui et al., 2014, 2016; Arrieta et al., 2011, 2017).

3. Methods

Facies analyses were performed using the guidelines provided by Collinson and Thompson (1982). Studied parameters include lithology,

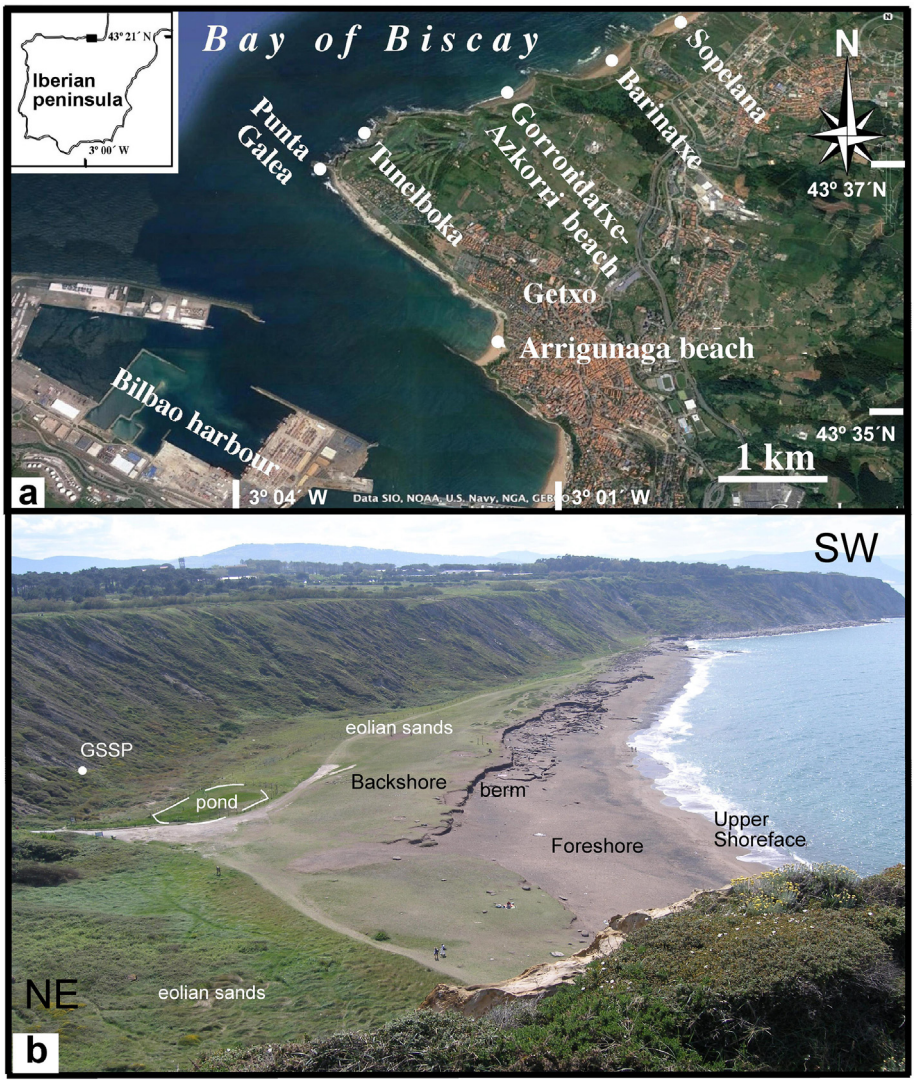

Fig. 1. Location of the studied beach in the northeast of Spain. **a:** The Gorrondatxe beach is located on the northeast coast of Spain, near Bilbao, a large industrial town with an important harbour; also shown are other, nearby locations and beaches mentioned in the study (the Tunelboka, Punta Galea and Arrigunaga beaches to the west; and the Barinatxe and Sopelana beaches to the east). b: View of the Gorrondatxe beach from the cliffs to the east of the beach, during low tide, showing the location of the sedimentary environments described in the text (backshore, foreshore and upper shoreface) and the presence of aeolian sands and ponds on the backshore. The location of the Ypresian-Lutetian Global Boundary Stratotype Section and Point (GSSP) is also shown. (For interpretation of the references to colour in this figure legend, the reader is referred to the web version of this article.)

grain size, texture, sedimentary structures, and the geometry of the strata.

Lithofacies were studied in many partial outcrops, with observations throughout the entire beach, for a complete 3-D study of sedimentary features. The study was combined with the construction of photomosaics in order to recognize the overall lateral and vertical facies variability, and the geometry of the strata following detailed bedding contacts. Digital analysis of images was used to increase the amount of data while keeping a high level of consistency across the data.

The various lithofacies were grouped into facies associations based on their spatial relations, attributed to specific depositional environments, and integrated into more general depositional settings. The sedimentological work was completed with an analysis of the vertical variability of grain-clast sizes. The type of interconnections among facies and the vertical stacking pattern of the facies associations revealed the aggradational and progradational trend for the studied beach as a whole.

A multi-temporal analysis of coastline changes during the last 65 years (1956–2021) was carried out utilizing historical and recent aerial photos from open repositories at the Spanish National Geographical Institute (Iberpix, http://www.ign.es/iberpix2/visor/) and the Basque country autonomous government (GeoEuskadi, https://www.geo.euskadi.eus/webgeo00-bisorea/es/x72aGeoeuskadiWAR/index.jsp).

More than twenty samples were selected to encompass the complete variety of different lithologies present in the beachrock, with at least one sample from each major beachrock zone for SEM analysis. The petrographic characteristics of the samples were studied by standard microscopy methods (both transmitted and reflected light) using Alizarin Red S and potassium ferricyanide staining (Dickson, 1965). Oriented thin sections were studied with a Nikon Labophot T2-Pol microscope coupled to a DS-L1 camera, the Nikon Eclipse E600 POL and the Leica MZ16 binocular magnifier equipped with a DFC 320 digital camera. A number of samples were selected and examined under a scanning electron microscope (SEM) and qualitatively determined (Al, Si, Fe, P, K, Ca) by energy-dispersive spectrometry (EDX) using a Jeol JSM 6400 at the University of the Basque Country.

A portion of the samples were ground and homogenized manually in an agate mortar, for analysis by powder XRD. The analyses were performed with a Phillips PW1710 diffractometer using Cu Ka radiation monochromated by graphite with generator conditions of 40 kV, 20 mA, a step size of 0.02° (°2θ) and a time per step of 1 s, at the University of the Basque Country. The specific software PANalytical X'pert HighScore,

in combination with the PDF2 database of the International Centre for Diffraction Data (ICDD), was used for the computer treatment of the obtained diffractograms and the identification of the present phases.

4. Results

4.1. Facies, sedimentary environments and facies model

The beach and beachrock sediments are subdivided into three sedimentary environments, based on lithology, bedding and sedimentary structures, and their location in relation to the current beach: a) upper shoreface, around the low-tide mark, and characterized by gravels and coarse sands with multidirectional trough and planar cross-stratification; b) foreshore, the area located in the main intertidal zone, mainly composed of sands with minor gravels; here swash and backwash wave action give rise to a distinctive low-angle, seaward-dipping, planar-parallel lamination of the sands, but the presence of major erosive bounding surfaces is remarkable; and c) backshore, an area with a mixture of marine sands (washover) and non-marine sands and muds (aeolian, subaerial ponds) in a topographically higher position, above the high-water level. No trace fossils were observed during the study, probably due to the severe environmental conditions (e.g., high-turbulence flows and swash and backwash processes in upper shoreface and foreshore respectively), continuously shifting substrates of gravels and coarse sands, the pollution related to the presence of slag, and their overall low preservation potential (Howard and Frey, 1984).

4.1.1. Upper shoreface

Upper shoreface beachrock deposits correspond to conglomerates and coarse-grained sandstones. When the beach is totally exposed at the spring low tide, they are located at or slightly above the lower water level. Five facies of massive to cross-bedded conglomerates, pebbly sandstone and coarse-grained sandstones are described and interpreted in Table 1 and shown in Fig. 2. These sediments do not show clear boundaries between the different facies; bedding is usually diffuse and vertical, and lateral gradations among the different facies are common. All these facies show a characteristic, whitish, circumgranular aragonite cement. The conglomerates (Facies Gms, Gpl and Gpc; Fig. 2a–d Table 1) are poorly to moderately-sorted, clast- or matrix-supported, containing rounded to well-rounded, spherical to disc-shaped, pebbles to cobbles of variable size and nature. A mixture of anthropic clasts (mainly derived from carbonate flux and metallic slag, including anthropic artefacts such as bricks; Fig. 2g) and locally derived clasts is common in these facies.

The sandstones are concave, tangential and sigmoidal cross-bedded, medium to coarse-grained sandstones (Facies Ssc; Fig. 2e); lamination is characterized by a centimetric alternation of coarse- and fine-grained laminae with granule layers and clasts dispersed in different laminae showing a preferred orientation of the long axes in accordance with the cross-bedding. Large, outsized clasts of the beachrock are included at the base of some beds (Fig. 2e). Asymmetric megaripples characterized by biconvex and rounded stoss sides with sigmoidal cross laminae are also present (Fig. 2f); they show erosive bases, mainly planar, but locally they can be similar to potholes with steep and vertical forms. Planar-laminated sandstones (Facies Spq; Fig. 2g), occasionally showing subtle undulation (quasi-planar lamination, sensu Arnott, 1993), are also found; these sandstones show no evidence of lateral accretion but only vertical aggradation, and their internal laminae concordantly drape the erosive, lower surface.

The upper shoreface is characterized by waves constantly breaking throughout each tidal cycle, so it is an area with high-turbulence flows. Related to these flows, wave winnowing removes all fine-grained sands and muds, but not the coarser sand fraction, at least near the boundary with the foreshore. Thus, beachrock upper shoreface facies are generally a mixture of gravels and sands, and the maximum clast sizes of the entire beachrock are found here, the sands in this zone being coarser than those in the nearby foreshore. Wave and current interactions can be highly complex in this zone, so the sedimentary structures in sand-dominated sediments are mainly composed of different kinds of cross stratification (dipping in all directions) and high energy parallel lamination. Large erosive surfaces are common between the different facies of the upper shoreface they are mainly planar, but locally they can be similar to potholes with steep and vertical forms (Fig. 2h).

4.1.2. Foreshore

The foreshore is confined to the intertidal zone, which is indicated by a sharp variation in slope, both at the base and top of the beachface. At the beachrock, five facies of sandstones and minor conglomerates are described and interpreted in Table 1 and grouped in two subassociations: channelled and non-channelled, the latter being the predominant one (Figs. 3–5).

The non-channelled beachrock subassociation mainly consists of low-angle planar-laminated sandstones (facies Spl; Figs. 3 and 4). This facies is composed of granule to fine-grained sandstone, forming laterally extensive sheets with wedge to planar, scoured erosive bases (Fig. 3a) and with well-developed parallel lamination (Fig. 3b). The lamination is characterized by a centimetric to decimetric alternation of coarse- and fine-grained laminae with granule and gravel layers (Fig. 3c and e), and gently dips uniformly (3°-7°) in a seaward direction, being parallel to the beach slope, whereas the strike of the lamination is parallel to the shoreline. Occasionally, the lamination is planar or with a slight landward dip; in close view it locally resembles cross-bedding, especially if other foresets dipping seaward are present (Fig. 3c, lower part; bed 3 in Fig. 4). At outcrop scale and in a wider view, however, the lamination is mainly planar (beds 3 to 6 in Fig. 4).

Pebbles and cobbles (up to 50 cm in diameter) are scattered throughout these sand beds (Figs. 3c and 4), including the larger boulders of the beachrock (bed 13 in Fig. 4), and sometimes lags one clast thick are also present at set boundaries. Additional sedimentary structures in these sandstones include wave-ripple lamination (Fig. 3d) and load structures (Fig. 3c).

Large erosive truncation and bounding surfaces are also recognized at the base of different beds (Fig. 3a and c; Fig. 4). These represent extensive, outcrop-scale, erosive surfaces, with local sedimentary interruption and a major sedimentary break; across these surfaces both the dip of the lamination and the grain sizes are clearly different (Fig. 4). The relief of these surfaces is up to 1 m in height, and they extend up to several tens to a hundred metres in length (Fig. 4). Two major kinds of surface are recognized, although this could be an observational bias: a) seaward-dipping, planar surfaces with the overlying stratification parallel to subparallel to the erosive surface, giving the outcrop a slightly wedge-shaped form (Fig. 3a); b) large, low-angle, undulating erosive surfaces, intersecting the lamination at higher angles (base of beds 7 and 12–13 in Fig. 4).

The beachrock channelled facies mainly consist of erosive, cross-bedded sandstones (Facies Sc; Figs. 4 and 5) with sharp, erosional basal boundaries (channels) and flat tops (Fig. 5a); various kinds of cross-bedding (trough, planar, locally sigmoidal) are the main sedimentary structures (Fig. 5a). Mud drapes (Facies Mm; Fig. 5b) and mud clasts as lags (Fig. 5c) are locally present.

Foreshore beachrock sandstones are mainly composed of the Spl facies. Laminations in this facies are interpreted as produced by swash and backwash processes associated with wave action in the foreshore. Within the Spl facies, low-angle erosive truncation surfaces clearly reflect periods of erosion related to subtle changes in the slope of the beachface, probably due to varying wave conditions during accretionary phases (Reinson, 1984; Pemberton et al., 2012). Because of their undulated shape (Fig. 4), they are interpreted as being a result of the presence of well-developed beach cusps on the foreshore. The development of beach cusps along the entire length of the Gorrondatxe foreshore has been observed and documented in aerial photographs and, as in other

Table 1
Facies description, suggested processes and environmental interpretation of studied sediments.

Facies	Description	Suggested processes and interpretation	Environment
Facies Gms: massive, clast-supported Conglomerates (Fig. 2a–b).	Poorly sorted, massive, clast-supported conglomerates. Clasts are usually rounded to disc-shaped, outsized boulders (up to 40 cm) of Paleogene limestones occur along the entire beach. Larger long-axis of clasts bear different orientations, even vertical regarding bedding. Coarse sandy matrix is also locally present. This facies is massive and ungraded, showing no internal structure, but crude horizontal lamination is locally developed. This facies, in the upper shoreface form beds of about 0.2–1.2 m in thickness; meanwhile in the foreshore, comprises thinner beds (up to 40 cm thick) and tends to display a lateral continuity of tens to hundreds of metres, pinching out laterally. Within a single bed, and laterally, the amount of gravel-size clasts decreases, locally changing to a pebbly sandstone deposit and then pebbles and boulders disappear with only the sandy portion of the bed remaining. Basal boundaries are diffuse and slightly erosional.	The Gms facies results from rapid gravel deposition from non-confined and turbulent flows. Its mostly clast-supported nature indicates that the flows were highly concentrated and poorly confined, and that the clasts remained closely packed during deposition, during which the massive settling of the sediment load prevented the development of bedforms (Fisher, 1971). "Plunge step" deposits close to the low-water level on modern conglomerate beaches (Hart and Plint, 1989, 1995; Hiroki and Terasaka, 2005).	Upper shoreface/Foreshore
Facies Gpl: parallel-laminated Conglomerates (Fig. 2a–c).	Moderately sorted, clast- to matrix-supported conglomerates; when the medium to coarse-grained sand is abundant it can be considered a pebbly sandstone. Dominant sedimentary structure is a planar, parallel-lamination; it is ungraded with alternation of laminae of different sizes; although inverse grading has been locally observed. Individual clasts show imbrications and a preferred orientation of the long axes. Basal boundaries are diffuse or slightly erosional.	The Gpl facies shows a combination of features usually associated with turbulent-flow deposits (e.g. poor sorting and a slightly erosive base), as well as features of stream-flow deposits (e.g. clast subrounding and clast imbrications). This facies is attributed to high-energy, shallow-water sheet and tractive flows in the upper shoreface; inverse-graded units resemble sieve deposition (Todd, 1989). "Plunge step" deposits close to the low-water level on modern conglomerate beaches (Hart and Plint, 1989, 1995; Hiroki and Terasaka, 2005).	Upper shoreface
Facies Gpc: planar, cross-bedded Conglomerates (Fig. 2d).	Planar, cross-bedded, clast- to matrix-supported conglomerates; cross-beds show multiple dipping directions, but mainly seawards. Planar cross-bedding is sometimes diffuse and clast orientations in Gpc facies also resemble Gpl facies with a gradual transition between both facies.	The tabular cross-beds of the Gpc facies record the presence of gravelly dune bedforms, originated by bedload sedimentation from unidirectional flows as indicated by the presence of cross-bedding. Migration of gravel bars with well-developed slipfaces at the "plunge step" close to the low-water level on modern conglomerate beaches (Hart and Plint, 1989, 1995; Hiroki and Terasaka, 2005).	Upper shoreface
Facies Ssc: sigmoidal, cross-bedded Sandstones (Fig. 2e–f).	Concave-, tangential- and sigmoidal-cross bedded, medium to coarse-grained sandstones. Lamination is characterized by a centimetric alternation of coarse- and fine-grained laminae with granule layers and clasts dispersed in different laminae showing a preferred orientation of the long axes according with the cross-bedding. Large outsized clasts of the beachrock are included at the base of some beds. Some forms characterized by biconvex and rounded stoss sides with sigmoidal cross laminae. Erosive bases are mainly planar, but having locally steep and vertical, pothole forms.	Facies Ssc are produced by bedload sedimentation from unidirectional flows as indicated by the presence of cross-bedding due to the migration of sandy asymmetric megaripples or small bars. Because of bedform lateral migration, deposits of the shoreface include erosion surfaces overlaid by cross-stratified sands.	Upper shoreface
Facies Spq: planar to quasi-planar laminated Sandstones (Fig. 2f).	Planar laminated sandstones, occasionally showing a subtle undulation; internal laminae concordantly draping the erosive, lower surface. Lamination is characterized by an alternation of coarse- and fine-grained laminae with granule layers and preferred orientation of clasts. Vertical and lateral gradation to Gpl facies has been locally observed.	No evidence of lateral accretion but only vertical aggradation (quasi-planar lamination, sensu Arnott, 1993); Planar or quasi-planar-laminated beds are usually related to high-energy combined flows produced by large-event storm sedimentation (Arnott, 1993).	Upper shoreface
Facies Spl: low angle, planar laminated Sandstones (Fig. 3a–d).	Granule to fine-grained sandstone, forming laterally extensive sheets with flat to planar, scoured erosive bases and with a well-developed parallel lamination; although occasionally there are some massive beds. Lamination is characterized by a centimetric alternation of coarse- and fine-grained laminae with granule layers and preferred orientation of clasts at the base of some levels. The low angle planar lamination gently dips uniformly (3°–7°) in a seaward direction; being parallel to the beach slope, meanwhile the strike of the lamination is parallel to the shoreline. Occasionally, lamination is planar or with a slight landwards dip; in a close view it locally resemble a cross-bedding, especially if other foresets dipping seawards are present. Pebbles and cobbles (up to 50 cm in diameter) are scattered throughout these sand beds, including larger boulders of the beachrock and, sometimes lags one clast thick are also present at set boundaries. Additional sedimentary structures in these sandstones include wave-ripple lamination with a wavelength of 10–15 cm and a typical height of several centimetres and load structures. Large truncation and bounding erosive surfaces have been also recognized at the base of different bed groups.	Swash stratification marked by variations in the grain size of sand and related to plane bed sediment transport during swash-backwash processes related to wave action; this action is able of selectively sorting and uniformly spreading sediment into individual layers (McKee, 1957; Clifton, 1969). The presence of bed load structures reflects wave-induced liquefaction during storm activity (Pemberton et al., 2012). Low-angle, truncation, erosive surfaces reflect periods of erosion related to subtle changes in the slope of the beachface probably due to varying wave conditions during accretionary phases originated by the presence of well-developed beach cusps on the foreshore. As beach cusps are very dynamic forms and change rapidly over time, the presence of these truncation surfaces constitutes clear evidence for their erosive origin probably as cusp mounds, which are characterized by parallel planar beds representing accretion deposits, whereas scour appears to be mostly concentrated in the troughs among cusp mounds (Komar and Holman, 1986; Holland and Elmore, 2008).	Foreshore
Facies Sc: channelled, cross-bedded Sandstones (Fig. 5a–c).	Medium- to very coarse-grained, moderately sorted, sandstones. They have sharp and erosional basal boundaries (channels) and flat tops; different kind of cross-bedding (trough, planar, locally sigmoidal) are the main sedimentary	High-energy and rapid bed-load deposition of sands and gravels as channel-bars in channels from unidirectional currents as indicated by the presence of cross-bedding. The small thickness of the channels suggests shallow channels	Foreshore.

(continued on next page)

Table 1 (*continued*)

Facies	Description	Suggested processes and interpretation	Environment
	structures. Laterally they are not very extensive (tens of metres) with maximum thickness up to 1.2 m. At the base of some sets, granules are present with scattered small pebbles. Mud clasts and mud drapes (Facies Mm) are locally present.	filled during waning flows, implying that high flow events were probably intermittent recording cut-and-fill processes (Collinson and Thompson, 1982). Gravels, as very thin deposits or as lags, are common overlying the large erosional bounding surfaces that form the bases of channel-fill units. Channelled facies clearly represent the development of rare, slightly incised channels in the foreshore. Similar channels have been widely described in modern beaches with a similar tidal range (Hori et al., 2002; Dalrymple and Choi, 2003), although they are uncommon on reflective beaches.	
Facies Mm: massive Mudstones (Fig. 5b).	Massive, light brown, mudstones. The thickness of this facies varies from some millimetres to 3 cm. They are located at the base of some sets within the channels as mud drapes, mantling even the vertical portions of the base of some sets. Erosion of this facies originates mud clasts embedded within Sc facies.	Mud drapes within channels. They occur as very thin layers even in the more steep lateral parts of the channels, probably due to the highly cohesive character of muds. The presence of a continuous channel-lining mud suggests that they were deposited in a subaqueous environment in a momentarily inactive, but flooded channel. The presence of mudstone drapes within Sc facies suggests a gradual rather than an abrupt final abandonment of the channels.	Foreshore
Facies Shl: Horizontal and irregular laminated Sandstones (Fig. 6a–c).	Well-sorted, fine to medium (rarely coarse) sands and sandstones with a well-developed irregular and mainly horizontal lamination; pebbles (up to 10 cm in diameter) are scattered throughout these sand beds, plastic remains can be also found in this facies. They form centimetric to decimetric, sheetlike sets (10 cm to 30 cm thick), with horizontal stratification; individual sets have erosive bases having minimal relief (2–3 cm), and planar, irregular, parallel lamination at the base and massive tops. Locally, sets with very low-angle laminations have been also observed. Deformation structures such as convolute bedding and load casts are very common in the basal laminated bases. Overall stratification and lamination is concordant and horizontal, both in strike and in cross-section; although minor groups of laminae gently dip (<5°), east or west, in the strike of the shoreline.	The Shl facies are interpreted as being a result of washover processes, either as laterally extended layers and sheets or rarely as small, lobate washover fans. Shl facies are interpreted as sheet floods deposits dominated by traction flow, giving rise to planar-laminated sediments generated during larger storm events, when the foreshore is bypassed and foreshore sands are deposited into a protected backshore (Hayes, 1967; Allen and Johnson, 2010). As they form the main facies in this area, they can be considered likely to represent an extensive washover flat or terrace (Reinson, 1984; Switzer and Jones, 2008; Allen and Johnson, 2010) covering the entire length of the back part of the beach; occasionally, they formed washover fans, whose ends are recorded by the scarce low-angle laminations observed. Load structures and convolute laminae reflect wave-induced liquefaction related to rapid deposition of sands during storm activity (Pemberton et al., 2012).	Backshore (washover)
Facies Sm: fine-grained, massive Sands (Fig. 6c–d).	Massive, gray, homogeneous, fine-grained sands at top of backshore sediments. They can be found as small (western part of the beach) or large (eastern part of the beach) vegetated mounds or hummocks, or at the lower part of the cliffs (climbing sands). The sands are commonly extensively disturbed by root growth and may contain isolated gastropod shells.	Sm facies is interpreted as aeolian sand. These sands are commonly found in the surface at the top of the backshore terrace, above the high springtide mark, as in other backshore environments (Hesp, 1999). The small sandy mounds are usually called nebkhas (Cooke et al., 1993; Hesp, 1999), which are considered incipient foredunes due to sand deposition produced by the presence of some rough obstacles that quickly reduce wind velocities causing sand accumulation. In the eastern part of the beach, however, there are some larger forms that can be considered embryonic foredunes, but these are highly modified by tracks made by human access to the beach. Finally, regarding the aeolian influence on the beach, it is worth mentioning the presence of climbing sands, usually covered by sparse vegetation, on the Paleogene cliffs in this eastern area of the beach. Aeolian sediments are of limited development in this coastal system, despite the strong winds that prevail throughout much of the year. This probably reflects both the very short distance over which the wind can blow and the lower rate of sediment supply due to the presence of a small cliff at the border of the backshore.	Backshore (aeolian)
Facies Ml: laminated Muds (Fig. 6d).	Parallel laminated or massive, millimetric to centimetric thick, muds with light colour (cream, light brown), intercalated within Sm facies.	The lower grain size clearly indicates low-energy mud deposition in a calm and quiet environment. The current presence of a nearby pond suggests that the Ml facies is related to pond sedimentation in the backshore area.	Backshore (pond)

beaches, the reflective slope is important in the development of a cuspate morphology (Sherman and Bauer, 1993; Roep et al., 1998). It is also important to note the temporal implications of these surfaces, as laterally they may be subtle, apparently conformable surfaces in strike view. Thus, beds 7 and 13 in Fig. 4 are separated by several other beds (8 to 12), but laterally bed 13b rests conformably on bed 7b (see also, Fig. 12a, which is a lateral view of Fig. 4), lacking all the intermediate beds.

Within the beachrock channelled association, the predominance of cross-bedded sandstones (Sc facies) clearly indicates the migration and accumulation of dunes or 3D megaripples within shallow channels. In some channels, mud drapes occur as very thin layers even in the steeper lateral parts of the channels, probably due to the highly cohesive character of muds (Fig. 5b). Underlying the base of some channels, there is a thin layer of massive sands (Fig. 5a, b). At first sight, these massive sands could be related to the formation of the channels. The absence, however, of a clear erosive surface at the base of the massive sands, together with the presence of gravel-sized clasts within the massive sands that could be related to single layers of gravel within the Spl facies (Fig. 5b), suggests that some kind of homogenization or destruction of the sedimentary structures took place as a result of the channel incision.

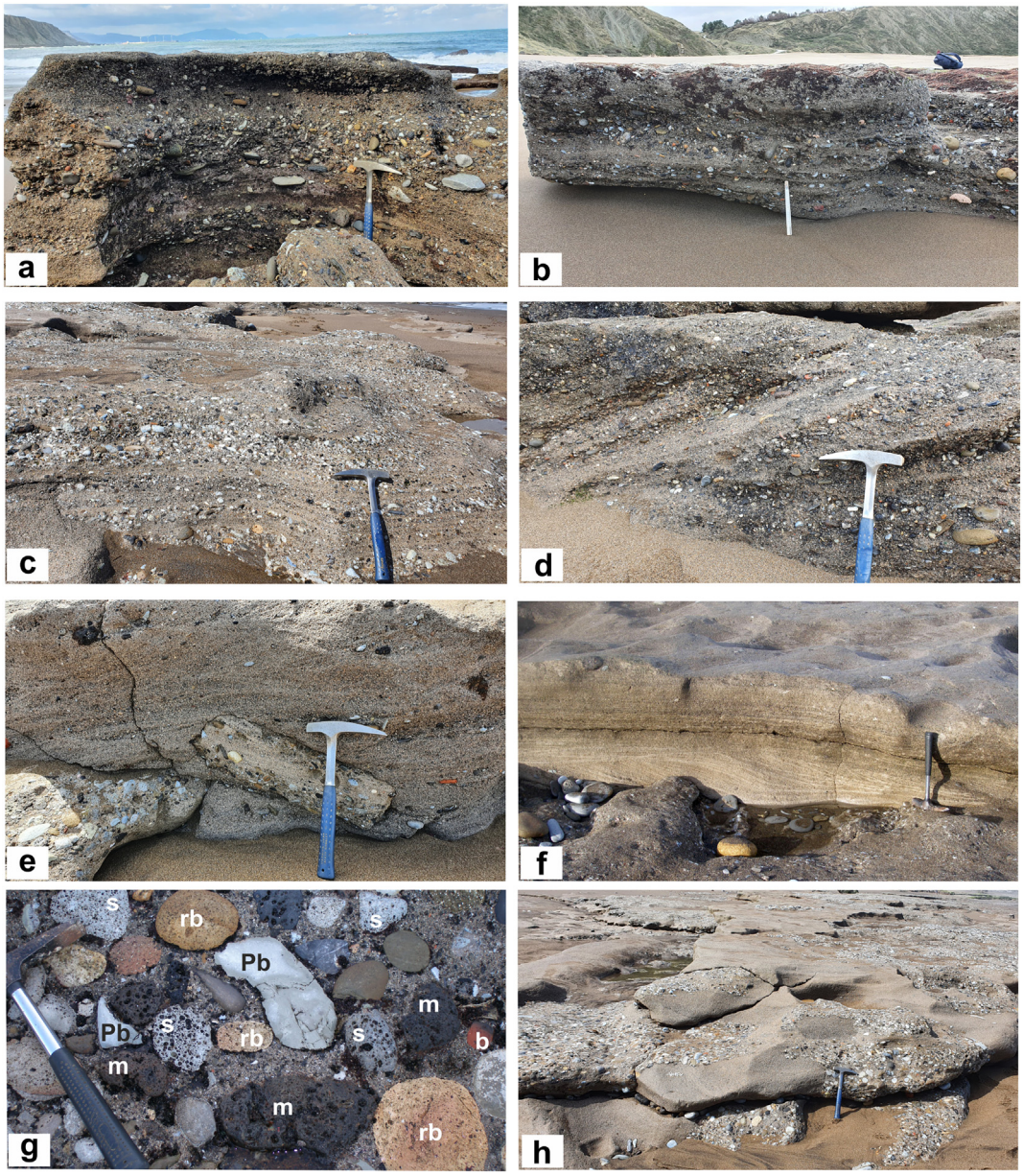

Fig. 2. Facies of the upper shoreface (see Table 1 for facies description). a–b: Massive clast-supported conglomerates (Facies Gms) and parallel-laminated conglomerates (Facies Gpl). c: Parallel-laminated conglomerates and pebbly sandstones (Facies Gpl). d: Planar, cross-bedded conglomerates (Facies Gpc). e: Sigmoidal cross-bedded sandstones (Facies Ssc) with a large, outsized clast from the beachrock included at the base. f: Sigmoidal cross-bedded sandstones (Facies Ssc) overlaid by planar to quasi-planar laminated sandstones (Facies Spq). g: Detail of anthropic slag-bricks (m: dark metallic slag, s: flux slag with vacuoles, rb: refractory bricks, b: red bricks and Pb: Paleogene blocks). h: Complex interrelationships between gravels and sandstones with several erosive surfaces, even vertical (left of the hammer). Hammer for scale in a, c, d, e and h is 33 cm long; stick for scale in b is 24 cm long. Hammer for scale in f and g is 40 cm long. (For interpretation of the references to colour in this figure legend, the reader is referred to the web version of this article.)

4.1.3. Backshore

The backshore corresponds to the supratidal zone. A berm, a change in slope, separates the backshore from the foreshore. Sedimentation in the backshore occurs above the mean high-water level, and temporal fluctuations between fresh and saline water are common. Wave and storm processes generally predominate during spring tides and storm surges, whereas aeolian and other sedimentary processes predominate the rest of the time. Three facies of beachrock sandstones and mudstones are described and interpreted in Table 1.

The beachrock backshore is mainly composed of well-sorted, fine to medium (rarely coarse) sands and sandstones, with well-developed, irregular and mainly horizontal lamination (facies Shl; Fig. 6a–c). Pebbles (up to 10 cm in diameter) are scattered throughout these sand beds, and plastic remains can also be found in this facies. The sand beds form centimetric to decimetric, sheetlike sets (10 cm to 30 cm thick), with horizontal stratification; individual sets have erosive bases with minimal relief (2–3 cm), and planar, irregular, parallel lamination at the base and massive tops. Locally, sets with very low-angle laminations have also been observed (Fig. 6b). Deformation structures such as convolute bedding and load casts are very common (Fig. 6a–c). Overall stratification and lamination are concordant and horizontal, both in strike and cross-section, although minor groups of laminae gently dip (<5°) east or west (Fig. 6b), in the strike of the shoreline. As they form the main facies in this area, they can be considered likely to represent an extensive washover flat or terrace (Reinson, 1984; Switzer and Jones, 2008; Allen and Johnson, 2010) covering the entire length of the back part of the beach. The upper surface of the washover terrace is a flat-lying to landward-sloping area, which can be considered the continuation of the berm crest. This surface is characterized by the presence of subaerial, predominantly wind-generated mounds and small

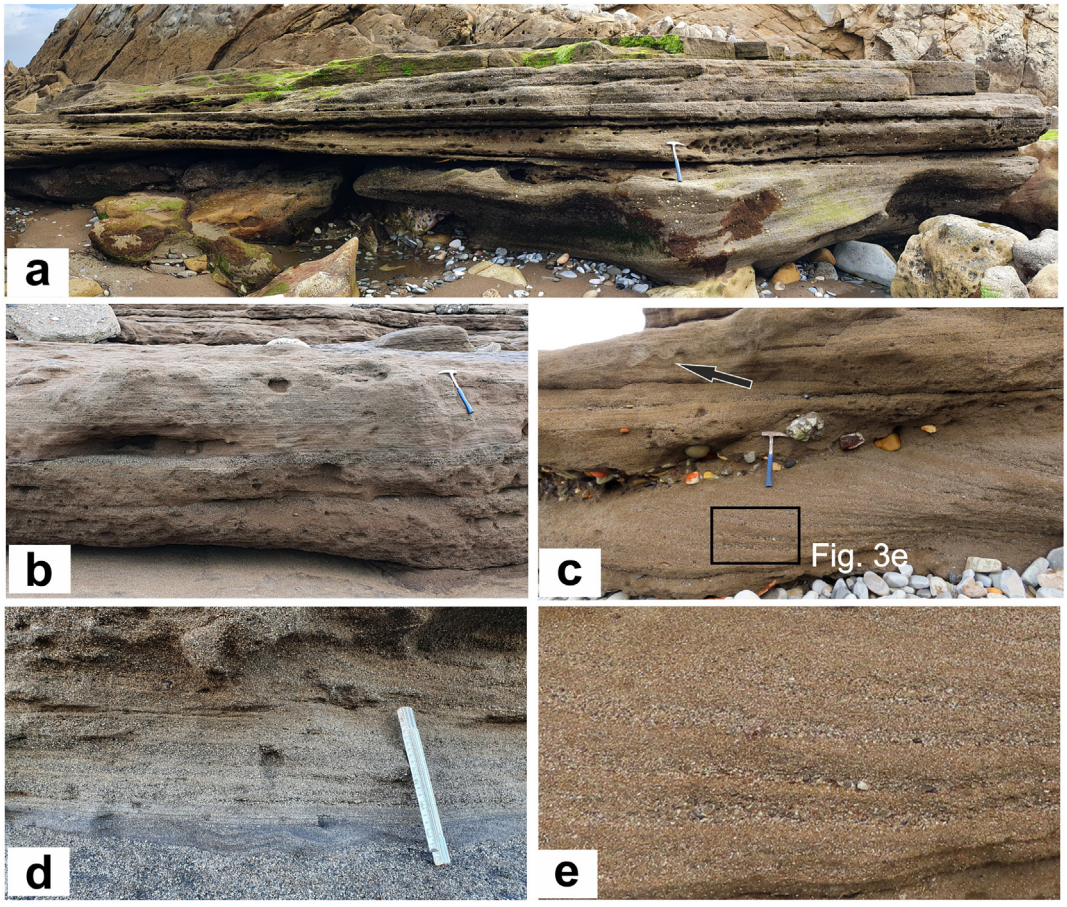

Fig. 3. Non-channelled facies of the foreshore (see Table 1 for facies description). a: Seawards (left), low-angle, wedge-shaped bedding characteristic of the Spl foreshore facies. b: Massive granule and parallel-laminated sandstones (Spl facies). c: Low-angle, planar-laminated sandstones of the Spl facies showing a gentle dip (3°-7°) in a seaward direction (left), with load structures (black arrow) present at the top of the outcrop. At the base of the outcrop, the lamination shows a slight landwards dip, which, in a close view such as this, locally resembles cross-bedding, especially if other foresets dipping seawards are present (see Fig. 4 for a more general view of this point). A thin conglomerate layer mantling a large erosive truncation surface is in the middle of the image. d: Wave-ripples within the Spl parallel-laminated facies. e: Detailed view of the lamination in panel c; centimetric to decimetric alternation of coarse- and fine-grained laminae with granule layers and preferred orientation of clasts at the base of some laminae. Hammer for scale in a, b and c is 33 cm long; stick for scale in d is 24 cm long. (For interpretation of the references to colour in this figure legend, the reader is referred to the web version of this article.)

ponds (Fig. 1b), whose sediments (Facies Sm and Ml; Fig. 6c–d) can be seen at top of the Shl facies.

Some massive sandstone sheets intercalated within the Shl facies might be older aeolian deposits that were later eroded by storm surges giving rise to the Shl facies (Fig. 6c). This backshore stratification could thus be the result of wave and aeolian sedimentation with sand accumulation on the upper surface of the washover terrace.

XRD analysis of the muds in the ponds (Fig. 1b), the mud drapes in the channelled facies of the upper foreshore (Fig. 5b), and Facies Ml of the backshore (Fig. 6d) revealed a strictly similar composition of illite, calcite and quartz minerals (Fig. 7), clearly suggesting a similar origin for these muds, very probably the Paleogene turbiditic sediments of the nearby cliffs.

4.1.4. Facies model

A facies model was developed for the beachrock at the extreme west of the beach (Fig. 8), where a complete section of the beachrock can be seen, showing the presence of the different beachrock zones superimposed upon each other in a single, composite section. In this area, Fig. 4 show an almost complete facies sequence of the beachrock. Only the top of the underlying upper shoreface beachrock deposits is visible, but they can be studied both laterally and at the rear of the Fig. 4 point of view, where several outcrops belonging to the upper shoreface deposits can also be studied and logged.

Gorrondatxe is characterized by maximum tidal amplitudes of about 4.3 m, with mean tidal ranges of 3 m. Wave processes dominate the system all year round, with the maximum wave height ranging from 11.9 m (January) to 4.9 m (June) and significant wave heights (i.e., the average height of the highest one-third of all waves measured; Blavette et al., 2014) ranging from 6.7 (March) to 2.7 m (June) (data from the Abra-Ciervana buoy, near Bilbao harbour, from the period 2001–2020; a table with buoy data for this period can be seen in Elorza, 2021). Coastal processes are thus dominated by waves crossing the beach-shoreface with the rising and falling tides. The model shows the aggradational and progradational structure of the different beachrock zones. Grain size decreases in the landward direction, and the model thus shows an overall fining-upward trend from the conglomerates at the upper shoreface at the low-water tide mark to the fine-grained sands and muds of the backshore area.

The different processes are preserved through the coastal areas, with the different beach and beachrock zones being dominated by distinct sedimentary structures (high-angle cross-bedding and quasi-planar-laminated beds at the upper shoreface; low-angle seaward-dipping stratification at the upper foreshore; and parallel lamination and low-angle cross-lamination at the backshore; Fig. 8). Data and sedimentary structures suggest that this system is more analogous to wave-dominated beach-shorefaces, probably with some tidal modulation (Dashtgard et al., 2021), as suggested by the mesotidal range. Moreover, the beach is affected by numerous storms, and this storm influence is

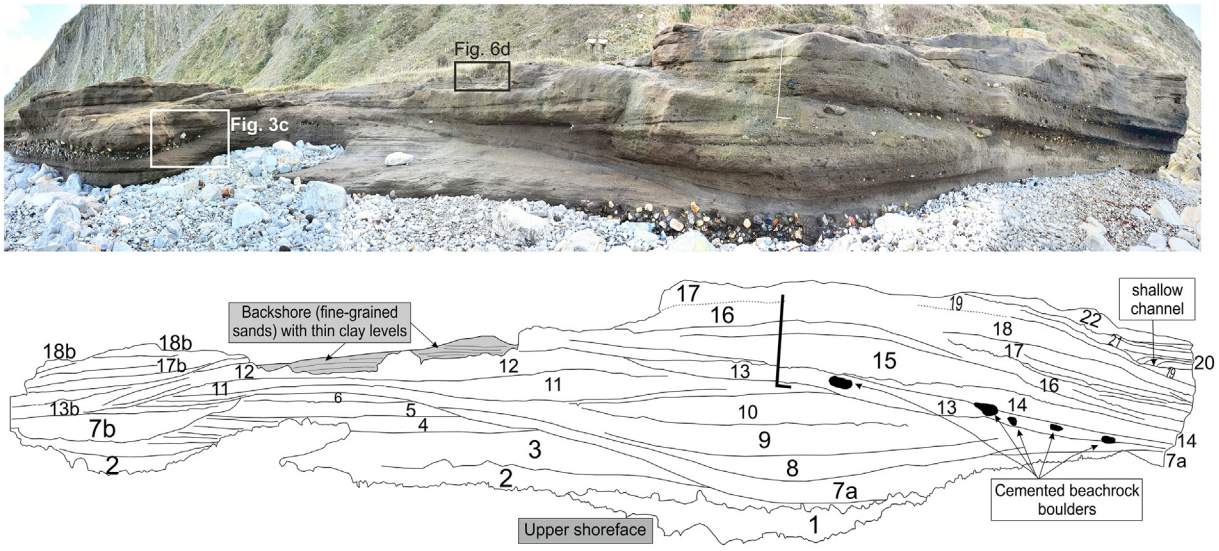

Fig. 4. Panoramic view and sedimentary interpretation of foreshore facies at the eastern end of the beach. Low-angle, planar-laminated sandstones of the Spl facies predominate (see Fig. 3 for detailed views); the lamination is characterized by a centimetric to decimetric alternation of coarse- and fine-grained laminae with granule layers. The low-angle planar lamination gently dips uniformly (3°–7°) in a seaward direction. Occasionally, the lamination is planar or with a slight landwards dip. Pebbles and cobbles (up to 50 cm in diameter) are scattered throughout these sand beds, including larger boulders from the beachrock (right), and sometimes lags one clast thick are also present at set boundaries. Large, erosive truncation and bounding surfaces are clearly recognized at the base of different bed groups (7, 13 and 15). A shallow channel is at the right of the outcrop. Basal upper shoreface facies (base, bed 1) and backshore facies (top) can also be seen in this outcrop. The facies model of Fig. 8 is derived from this outcrop. Large stick for scale is 1 m long. (For interpretation of the references to colour in this figure legend, the reader is referred to the web version of this article.)

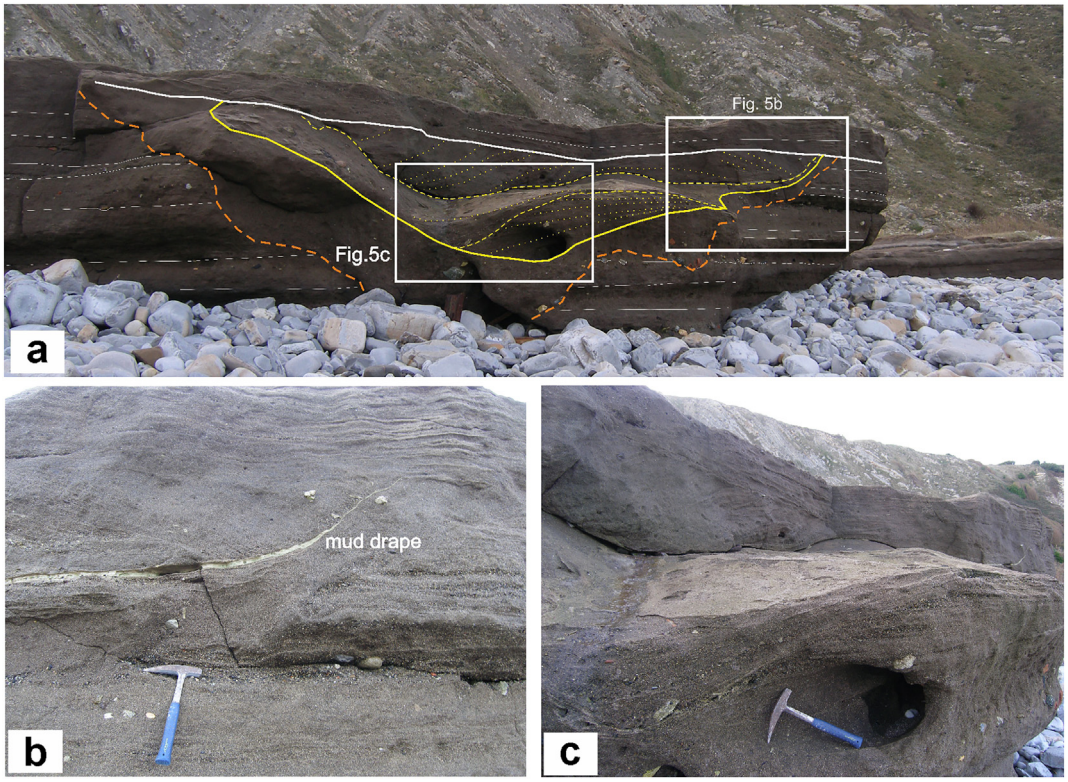

Fig. 5. Channelled facies of the foreshore (see Table 1 for facies description). a: Panoramic view of the medium- to very-coarse-grained channelled sandstones, showing sharp and erosional basal boundary (continuous yellow line) and flat top (continuous white line); different kinds of cross-bedding (trough, planar, locally sigmoidal) and internal erosive surfaces are the main sedimentary structures (dotted yellow lines). Below the channel, a thin layer of massive sands develops, parallel to the channel base (continuous orange line); this is the Spl facies, lacking any sedimentary structure. The absence of a clear erosive surface at the base of the massive sands, and the presence of gravel layers in continuity with similar layers of gravels within the Spl facies, suggests the existence of sedimentary homogenization or destruction related to the channel incision. b: Detailed view of the upper, right part of panel a; a thin mud drape mantles the bottom and lateral part of the channel; cross bedding is seen overlying the mud drape, and massive, homogenized sands underlying the mud drape. c: Detailed view of the basal part of the channel with erosive surfaces and cross bedding; several mud clasts can also be seen at the base of the channel (left of the hammer, which is 33 cm long). (For interpretation of the references to colour in this figure legend, the reader is referred to the web version of this article.)

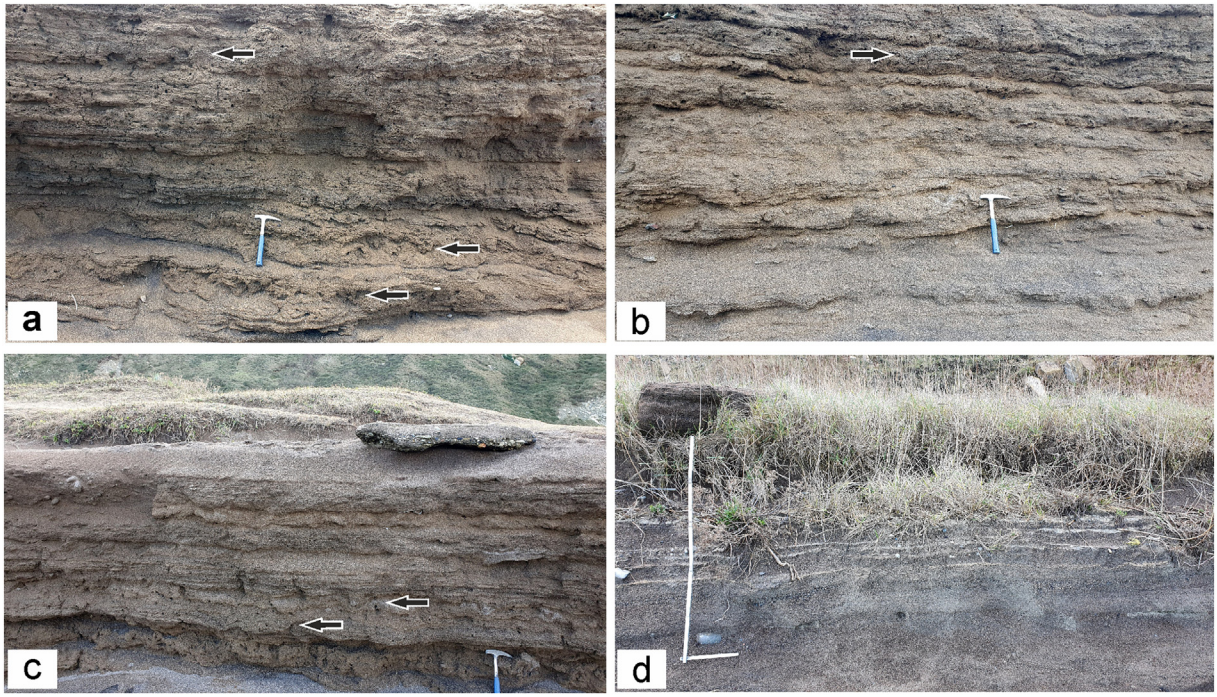

Fig. 6. Facies of the backshore (see Table 1 for facies description). a–b: Well-sorted sands and sandstones of the Shl facies, with a well-developed, irregular and mainly horizontal lamination. They form centimetric to decimetric, sheetlike sets (10 cm to 30 cm thick), with horizontal stratification (a); individual sets have erosive bases showing minimal relief (2–3 cm), and planar, irregular, parallel lamination at their base and massive tops. Locally, sets with very low-angle laminations have also been observed (b, close to the hammer). c: Sands and sandstones of the Shl facies overlaid by massive, homogeneous aeolian sands (Sm facies) forming vegetated mounds (nebkhas) at the top of the backshore sediments (a large block of recently eroded beachrock is also seen). d: Alternation of gray, aeolian sands (Sm facies) and thin, centimetric, whitish muds (Ml facies). Hammer for scale in a, b and c is 33 cm long; large stick for scale in d is 1 m long. Convolute lamination is common in this facies (some beds arrowed in a, b and c). (For interpretation of the references to colour in this figure legend, the reader is referred to the web version of this article.)

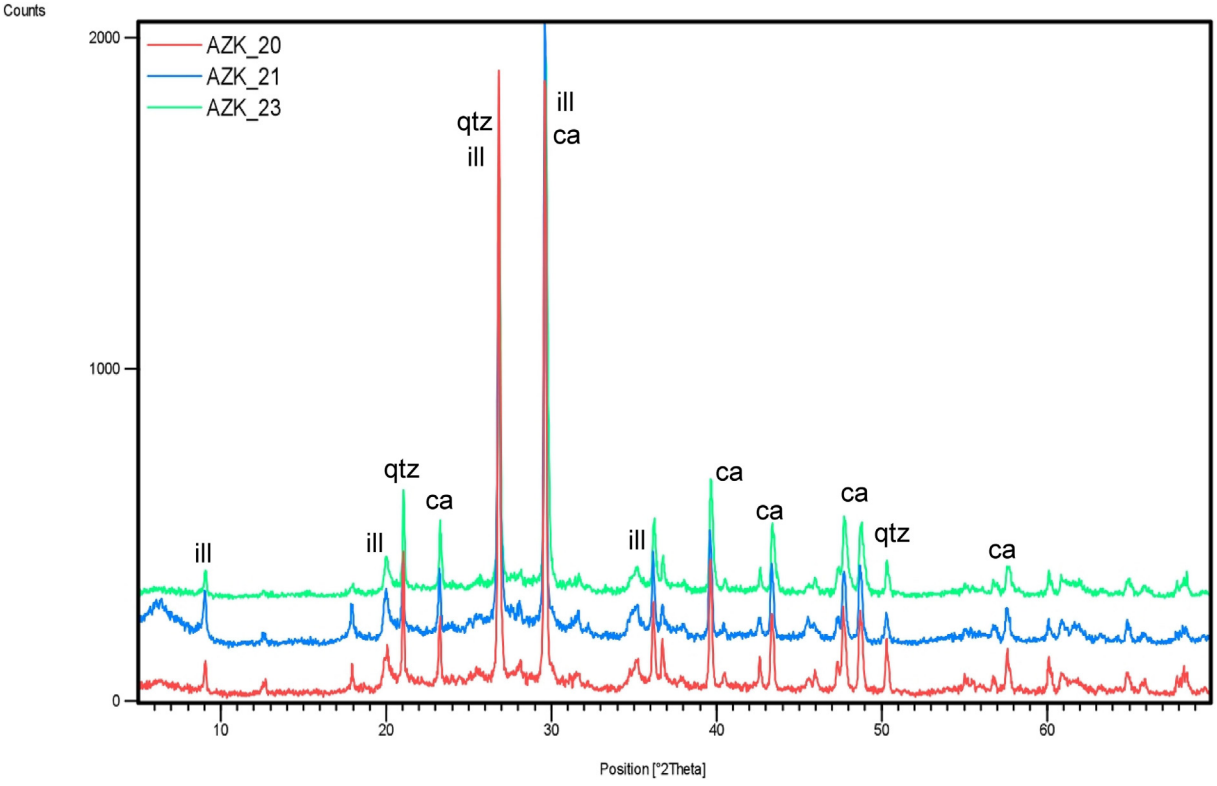

Fig. 7. XRD analysis of mudstone facies in pond (AZK_20) in the Ml facies of the backshore (AZK_21) and in mud drape of channels at the foreshore (AZK_23), showing exactly the same composition of illite (ill), calcite (ca) and quartz (qtz) as their major minerals.

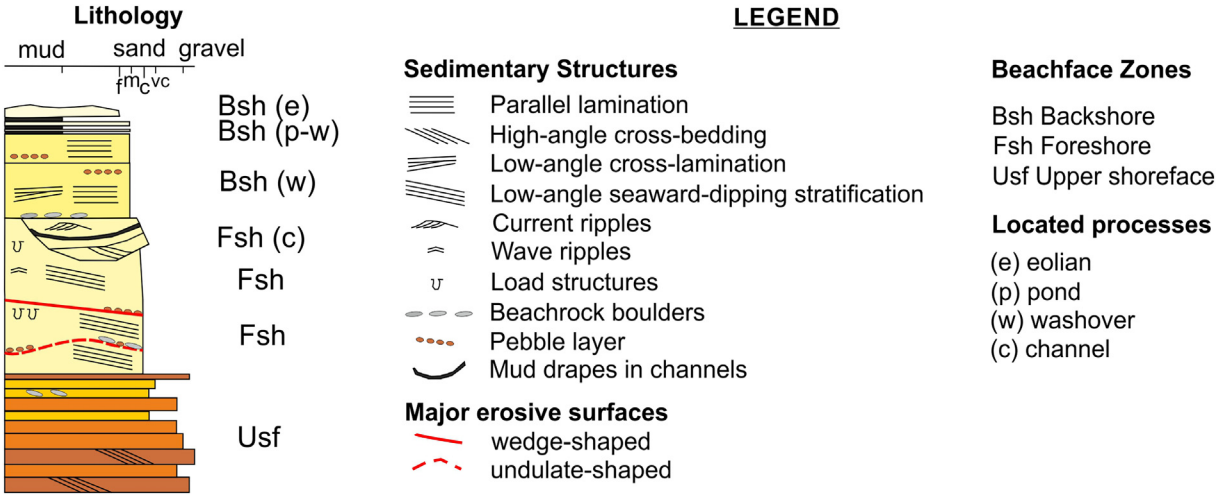

Fig. 8. Hypothetical facies model reconstruction of a preserved vertical profile based on the Gorrondatxe beach. The vertical scale is dependent on the tidal range (in this case ~3 m). The model also assumes that the system is aggradational and progradational, as shown in Fig. 4. The names of the beachface zones and the processes identified are also shown. (For interpretation of the references to colour in this figure legend, the reader is referred to the web version of this article.)

evident in the high turbulence associated with the conglomerate facies and Ssc-Spq facies of the upper shoreface and the presence of large erosive surfaces at the foreshore (Fig. 8), probably related to the development of beach cusps in that zone.

4.2. Beachrock cements

Regarding the beachrock development and sediment cementation of the Gorrondatxe beach, what is remarkable and up to now has not been considered or described in this particular area, is that the cementation is environmentally dependent, in the sense that the three beach zones bear their own features in their carbonate cements. The major components of cements, carbonate polymorphs, and the degree of cementation are different in the upper shoreface, the foreshore and the backshore zones.

4.2.1. Upper shoreface

In the upper shoreface zone, sediment cementation affects all the sedimentary facies described in Section 4.1.1. For simplicity and ease of treatment, only the sandstones of the sandy facies were studied, although the conglomerates and their sandy matrix show the same cementation pattern. The coarse sands of the Ssc and Spq facies include moderately sorted clasts and are composed of very coarse to medium sand sizes (1.5 mm to 0.3 mm). They are pervasively and strongly cemented, while maintaining a notable intergranular porosity. This cementation results in all these facies being strongly cohesive, and at first glance it is distinguished by its light tones compared to the darker facies of the other zones.

The sandy fraction in this zone (Fig. 9a–c) is composed of the following: bioclasts (b in Fig. 9a and c) such as echinoderm spines, bivalves, gastropods and red calcareous algae (stained with Alizarin Red S; Fig. 9a–b), with evidence of reworking and high roundness; terrigenous quartz (q in Fig. 9a and c), as extra clasts with a clearly bimodal size relationship, both monocrystalline and polycrystalline, with undulating extinction, the larger ones (>2 mm) rounded and the smaller ones (<0.2 mm) more angular (feldspar fragments are not recognized, although they are detected by XRD); rounded fragments of metallic iron oxide slag (m in Fig. 9a and c), which, according to the XRD analysis, correspond to goethite (FeOOH), magnetite (Fe_3O_4), haematite (Fe_2O_3) and wüstite (FeO); rounded fragments of slag from the limestone-dolomite flux (f in Fig. 9a and c) used in the blast furnace, with numerous vacuoles. The limestone flux has been transformed into pseudowollastonite ($CaSiO_3$) and gehlenite-akermanite Ca_2 ($Mg_{0.5}$ $Al_{0.5}$) ($Si_{1.5}$ Al $_{0.5}$ O_7) according to the XRD analysis and, due to its Ca content, is stained in a pink that is clearly different from the more intense red staining observed in the molluscan bioclasts. There are also clasts that behave isotropically, which are considered vitrified remains of the fluxes.

The dominant cement is made up of a well-developed drusy circumgranular aragonite with long, fine needles that surround the surface of all the clasts perpendicularly (Fig. 9a–d). Under SEM, a basal growth of micritic aragonite (m.a; Fig. 9e) crystals is visible, passing irregularly, without a clear boundary, to well-developed aragonite crystals (a, Fig. 9e–f); in spite of its small size at microscope view, this basal growth is a characteristic micritic black rim that is visible in contact with the clasts (Fig. 9a–c), passing to the circumgranular aragonite crystals (m.a to a in SEM view, Fig. 9e). The micritic aragonite is irregular in its development, 1–2 μm in length, whereas the aragonite crystals reach 80–100 μm in length and 2–3 μm in width. Irregular aggregates of iron oxides, clays and other materials, whose composition is difficult to determine due to their dimensions, are superimposed on the aragonite crystals (Fig. 9f). Under favourable conditions, bacterial forms also appear as nanometre-sized, spherical *Coccus*-type precipitates (cc in Fig. 9g–h), which are never larger than 100 nm, associated with each other as a bacterial community (clotted micrite) and with a tendency to become flattened and coated with carbonate. They are arranged in the protected zones between the surface of the clasts and the beginning of the micritic aragonite itself (Fig. 9g–h).

4.2.2. Foreshore

The facies of the foreshore zone are mainly sands, with a composition similar to those previously mentioned in the upper shoreface (bioclasts, quartz-feldspathic, slags of ores and carbonated fluxes). They show, however, an overall lower degree of cementation and greater intergranular porosity, and there are even small differences in the eastern zone (Fig. 10a–b) compared to the western zone (Fig. 11a–b) of the Gorrondatxe beachrock.

The recognized cementation is fundamentally meniscus-type (Fig. 10c), with a predominance of disordered, intercrossed and spaced needles of fibrous aragonite (a1 in Fig. 10c–e) that tend to form fans nucleating at separate points along the grain boundaries (Fig. 10d; Fig. 11c–d). They are never perpendicular to the clast surfaces. There are individualized and dispersed lepisphere-type (lp in Fig. 10d–e) mineral phases of small size (1 μm) of silicate composition (Fig. 10e), which are superimposed on the aragonite crystals, but can also cover organic ducts as branching-type filaments (Fig. 11e–g); they correspond to a magnesian silicate phase, as its main element, with traces of Al and Ca according to the EDX analysis. Other types of aggregate are *Bacillus*-type bacterial cells that are visible in free spaces (ba in Fig. 10g). Diatoms (Fig. 10f) and calcareous

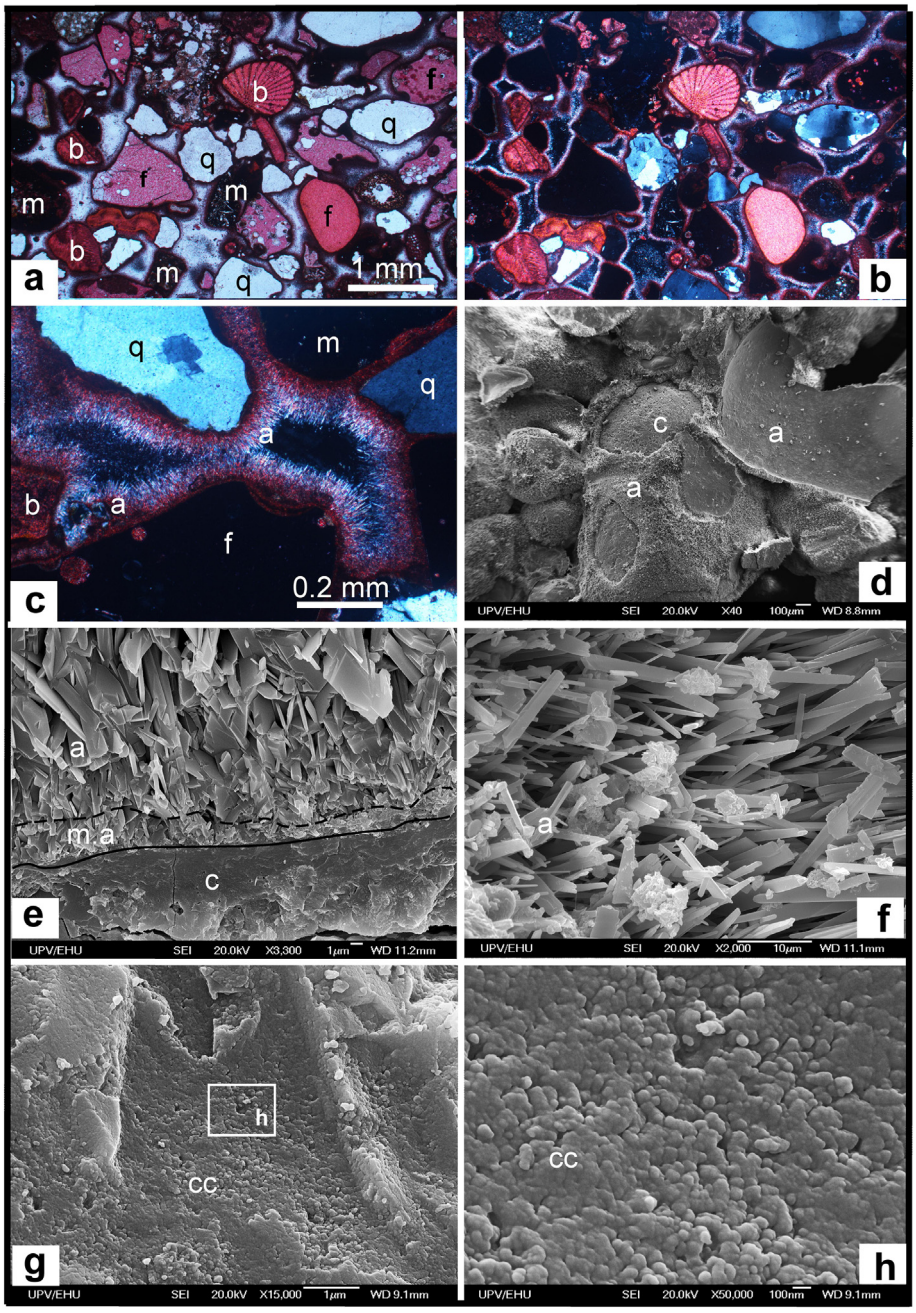

Fig. 9. Photomicrographs of the upper shoreface zone in the Gorrondatxe beach. a-b: General appearance of the bioclasts (b), quartz (q), flux slag with vacuoles (f), and metallic slag (m) grain-supported and cemented by circumgranular aragonitic cement; stained with Alizarin Red S; parallel and crossed nicols. c: Detail of the clasts cemented by a small dark micrite band followed by the growth of fine circumgranular aragonite needles (a); stained with Alizarin Red S; crossed nicols. d: SEM photomicrograph of the clasts (c) surrounded by an intense cementation of circumgranular aragonite crystals (a). e: SEM photomicrograph of the circumgranular aragonite cements (a) generated from a micritic aragonite cement (m.a), with irregular growth in contact with an undetermined clast (c). f: Detail of the well-developed aragonite prisms (a) with small aggregates of diverse compositions. g: Basal aspect of a cementation precursor (panel d) occupied by small nanospheres of bacterial origin, *Coccus*-type (cc). h: Detail of the nanospheres (*Coccus*-type) fossilized by carbonate. (For interpretation of the references to colour in this figure legend, the reader is referred to the web version of this article.)

algae (coccolithophores) occur as incorporated remains located on aragonite crystals (Fig. 10h). As in the upper shoreface, the presence of nanospherical *Coccus*-type bacterial forms in the basal clast-cement contact (cc in Fig. 11h) is also confirmed in the upper foreshore zone.

In this zone, the low-angle seaward-dipping lamination is mainly characterized by its darker tones. However, the presence of lighter laminations among the otherwise darker predominant laminations of the Spl facies is remarkable (Fig. 12a). Here, the presence of a notable meniscus cementation confers a greater resistance to weathering (Fig. 12b–d). The aragonite crystals (a1* in Fig. 12e–g), with a more compact prismatic habit different from the fibrous crystals with radial arrangements (a1 in Fig. 11c) (10–15 μm), are found mixed with smaller bladed (2–3 μm) calcite crystals (b.c; Fig. 12g) and occupy the spaces left by the predominant aragonite prisms, without interfering with the growth of the former (Fig. 12e–f). The core of the radial aragonite prisms corresponds to a clotted micrite set of nanospheres of bacterial origin (cc in Fig. 12g) that continues at the beginnings of the well-developed aragonite crystals. A carbonate patina (Fig. 12g) fossilizes all this bacterial component.

Moreover, the Spl facies locally encloses beachrock blocks (br1 in Fig. 13b; see also Fig. 4) belonging to the sandy facies of the upper shoreface that have been eroded, uprooted and transported to the foreshore (Fig. 13a–b). These blocks have undergone a double cementation,

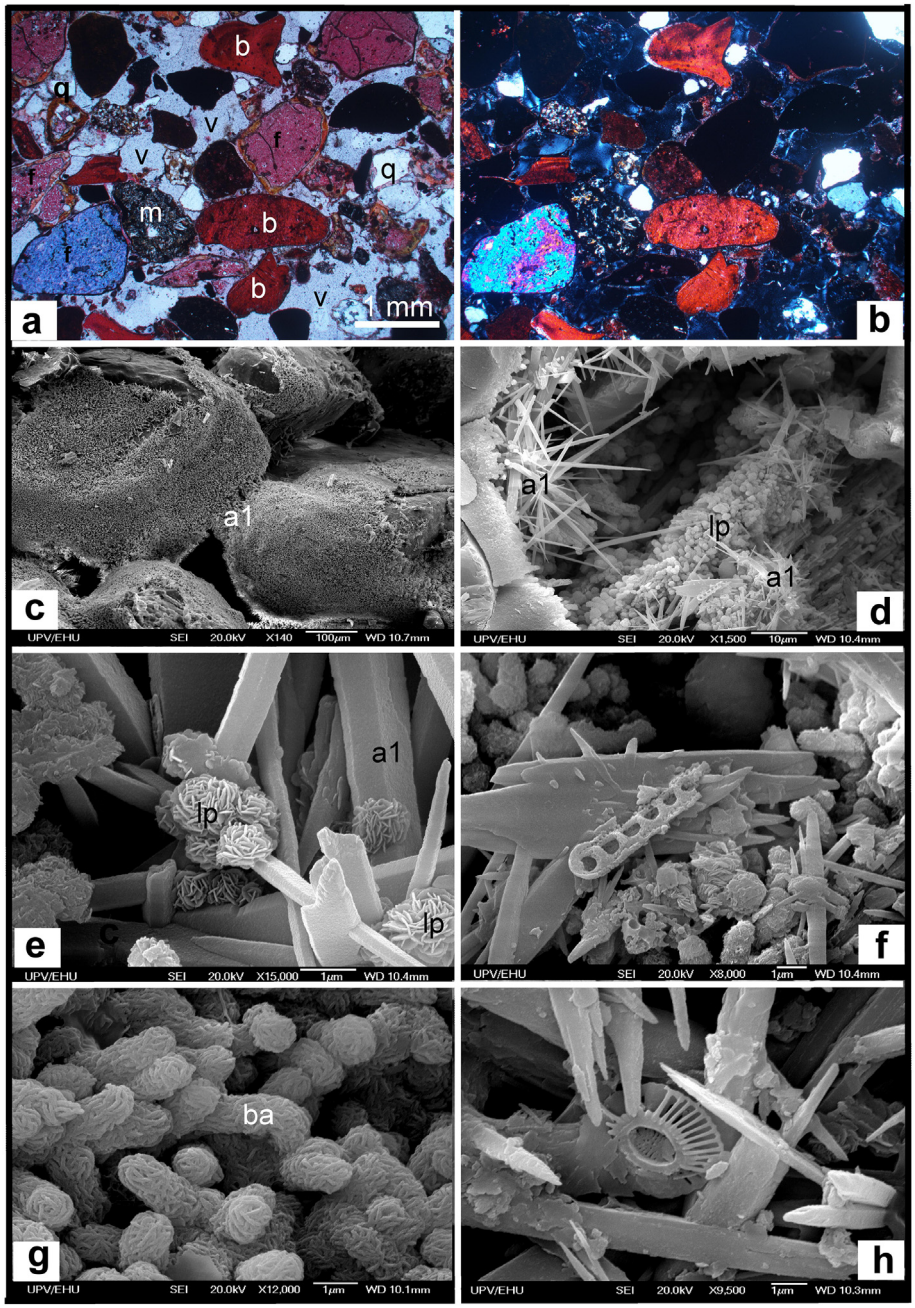

Fig. 10. Photomicrographs of the foreshore zone in the Gorrondatxe beach (eastern part). a–b: General appearance of the bioclasts (b), quartz (q), flux slag (f), and metallic slag (m) with large empty spaces (v), supported by imprecise cement. c: Clasts covered by aragonitic cement of acicular habit (a1), forming meniscuses and highlighting the maintenance of high porosity. d: Detail of the fine aragonite needles (a1) irregularly arranged with aggregates of lepispheres (lp). e: Groups of lepispheres (lp) of silicate composition, analysed by EDX, superimposed on well-developed aragonite prisms. f: Remnant of diatom frustule on aragonite crystals and silicate lepispheres. g: Set of bacterial organisms, *Bacillus*-type (ba), associated with each other forming elongated masses. h: Remains of calcareous coccolithophoric algae among the aragonite prisms. (For interpretation of the references to colour in this figure legend, the reader is referred to the web version of this article.)

superimposed and spaced in time, since they were first cemented in the upper shoreface, then eroded and deposited together with loose sands and other clasts in the foreshore (Fig. 13a) and cemented again. In these blocks, the first cementation of micritic aragonite (m.a in Fig. 13d) and circumgranular aragonite (a in Fig. 13d) distinctive of the upper shoreface, as already mentioned, is superimposed by the growth of other, finer aragonite prisms (a1 in Fig. 13d), arranged on top of the first ones and intergrown with each other, occupying empty spaces (Fig. 13c–d); the first fringe around beachrock clasts is totally preserved, as observed by SEM and conventional microscope. In addition, there is a precipitation of fine carbonate plates (p in Fig. 13e) (<5 μm) with no defined habit that belong to the cementation of this second stage. Apparent bacterial activity is widely represented by *Bacillus*-type bacterial cells (ba1 in Fig. 13g–h), which are clearly related to the strong corrosion observed in the first-generation aragonite prisms, where these rod-shaped forms seem to settle and develop intensively (Fig. 13f–h).

4.2.3. Backshore (washover facies)

The washover facies (Facies Shl) of the backshore is mainly composed of moderately to poorly sorted sands, close in composition to the sands in other studied zones. In this zone, however, there is a higher concentration of opaque, metallic ores; these opaque ores (goethite, magnetite, haematite and wüstite) are arranged in lamellae, which

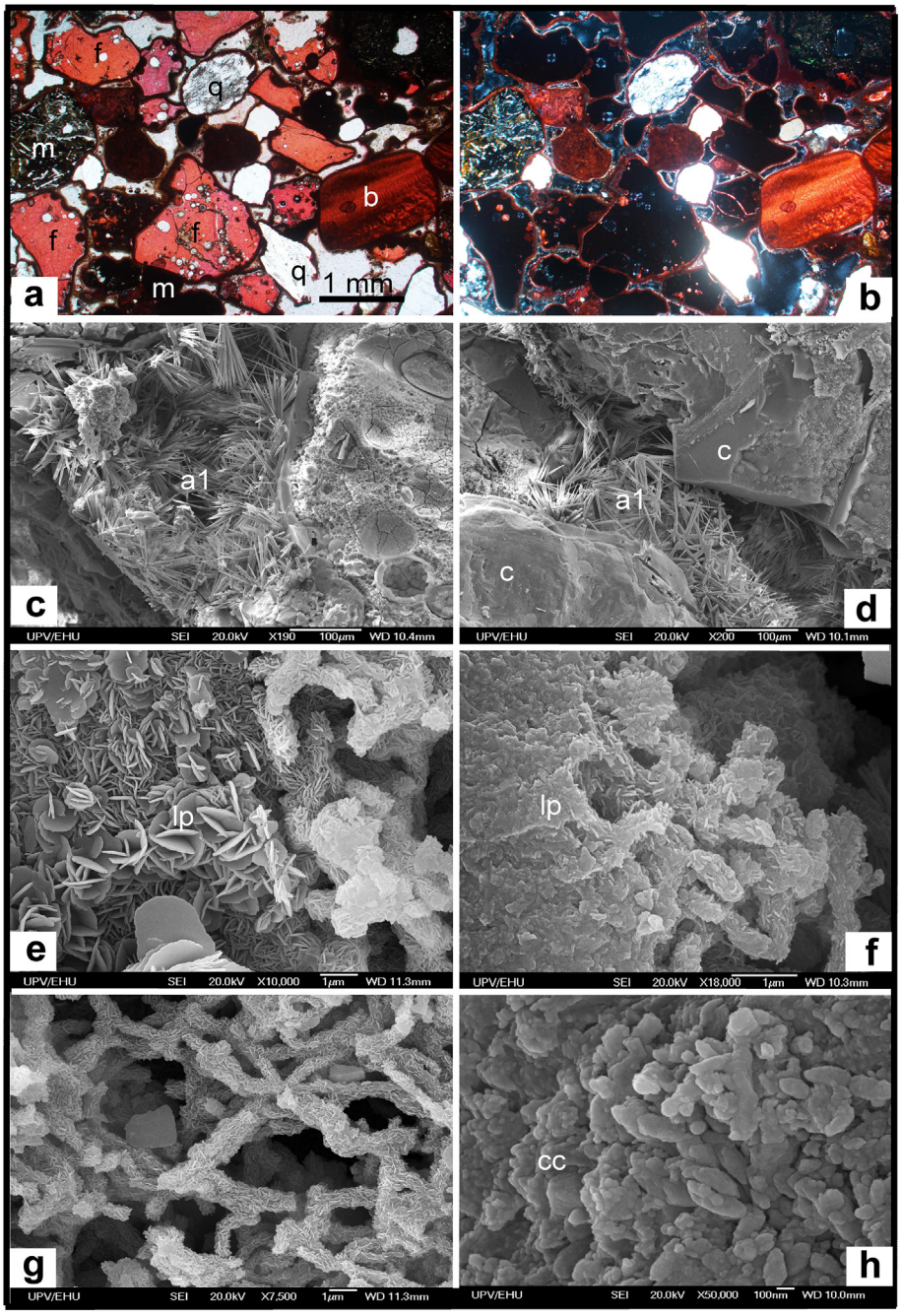

Fig. 11. Photomicrographs of the foreshore zone in the Gorrondatxe beach (western part). a–b: General appearance of the different types of clasts cemented by aragonite from a dark band of micrite. High porosity is maintained; parallel and crossed nicols, stained with Alizarin Red S. c–d: Different edges of flux slag cemented by fine aragonite needles arranged irregularly in a fan shape (a1). e–g: Simple lepisphere forms (lp), which go on to cover branching organic filaments. These filaments are unprecedented, unlike the bacterial assemblages found. h: Aggregates of *Coccus*-type nanospheres (cc) similar to those previously seen in Fig. 9g–h. (For interpretation of the references to colour in this figure legend, the reader is referred to the web version of this article.)

confer more intense, darker tones upon the sands and give a spongy appearance to the beachrock (Fig. 6a–b).

Its fabric is much less tight, with weak cementation produced on the grain edges (they can reach 150 μm in length along the grain contacts), thus maintaining a high porosity (Fig. 14a–b). This partial cementation shows a meniscus pattern, with two clear polymorphs; the more abundant one is formed by intercrossed aragonite needles (a2, Fig. 14c–d), slightly different from those found in the upper foreshore (a1 in Fig. 11c–d), whereas the less abundant one is formed by well-developed rhombohedral calcite crystals (r.c, Fig. 14e–f). The calcite crystals are euhedral and equigranular, and form individualized and/or grouped rhombohedrons in the flat areas of the clasts, with an average size of 7 μm, arranged on crystals of small aragonite prisms (Fig. 14g). The bacterial community is recognized by the presence of nanospheres (*Coccus*-type) (cc in Fig. 14h) of very similar size (100 nm) to the other zones. It is evident, then, that bacterial activity is also important in the washover deposits of the backshore (Fig. 14h).

5. Discussion

5.1. Cementation, facies and facies model

There are major differences in the facies cementation of the sands within the three zones of the beach. These differences are useful as a tool for distinguishing the sands in the presence of similar sedimentary

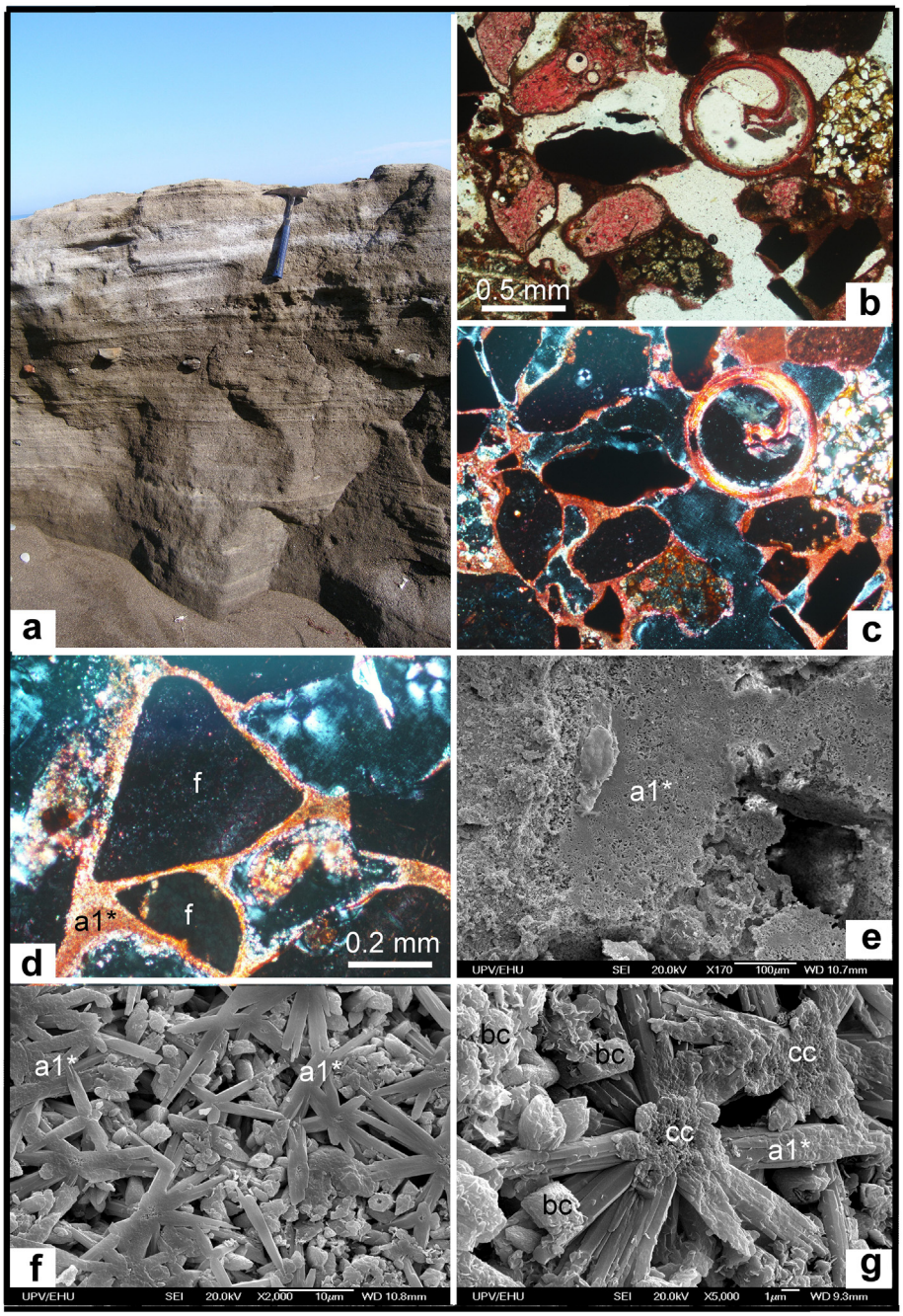

Fig. 12. Gorrondatxe foreshore zone with white laminations (western part). a: Foreshore appearance of dark tones with alternating laminations of lighter tones. Hammer length is 33 cm. b–c: View of the arrangement of clasts of varying nature with meniscus cementation; stained with Alizarin Red S; parallel and crossed nicols. d: Detail of several completely cemented clasts, but not circumgranular; stained with Alizarin Red S; crossed nicols; f, flux slag with vacuoles. e–g: At different scales, view of the basal surface of the cement in contact with the now detached clasts. The radial arrangement of the well-developed aragonite prisms (a1*) can be seen, together with small, bladed calcite crystals (b.c). The core of the aragonite prisms maintains nanospheres (cc) of bacterial origin as cementation triggers. (For interpretation of the references to colour in this figure legend, the reader is referred to the web version of this article.)

structures dominated by parallel-laminated sands. The upper shoreface sands show hard and well-cemented sandstones, good intergranular porosity, and whitish aragonite cement, whereas the foreshore sands show medium-hard and cemented sandstones, higher intergranular porosity, and brown irregular aragonite needle cement. The backshore (washover) sands show light cemented sandstones, the highest intergranular porosity, and brown aragonite together with rhombohedral calcite cements. At the upper shoreface-foreshore boundary, the sands of the Ssc and Spq facies (Fig. 2e–f) with whitish aragonite cement are considered to have been deposited in the upper shoreface, whereas the brown sands of the Spl facies (e.g. Fig. 3e) are considered to have been sedimented at the foreshore. In this case, the Spq and Spl facies show a very close and similar parallel lamination, at first sight, being distinguishable mainly by their different cementation. At the foreshore-backshore boundary, the differences are even more subtle because both have brownish colours. However, the parallel lamination of the Spl facies (foreshore) is more homogeneous (Fig. 3a and b), the rock being more consistent and harder due to its stronger cementation, whereas the parallel lamination of the Shl facies is more irregular (Fig. 6a–b), the rock being more friable and softer due to its lighter cementation.

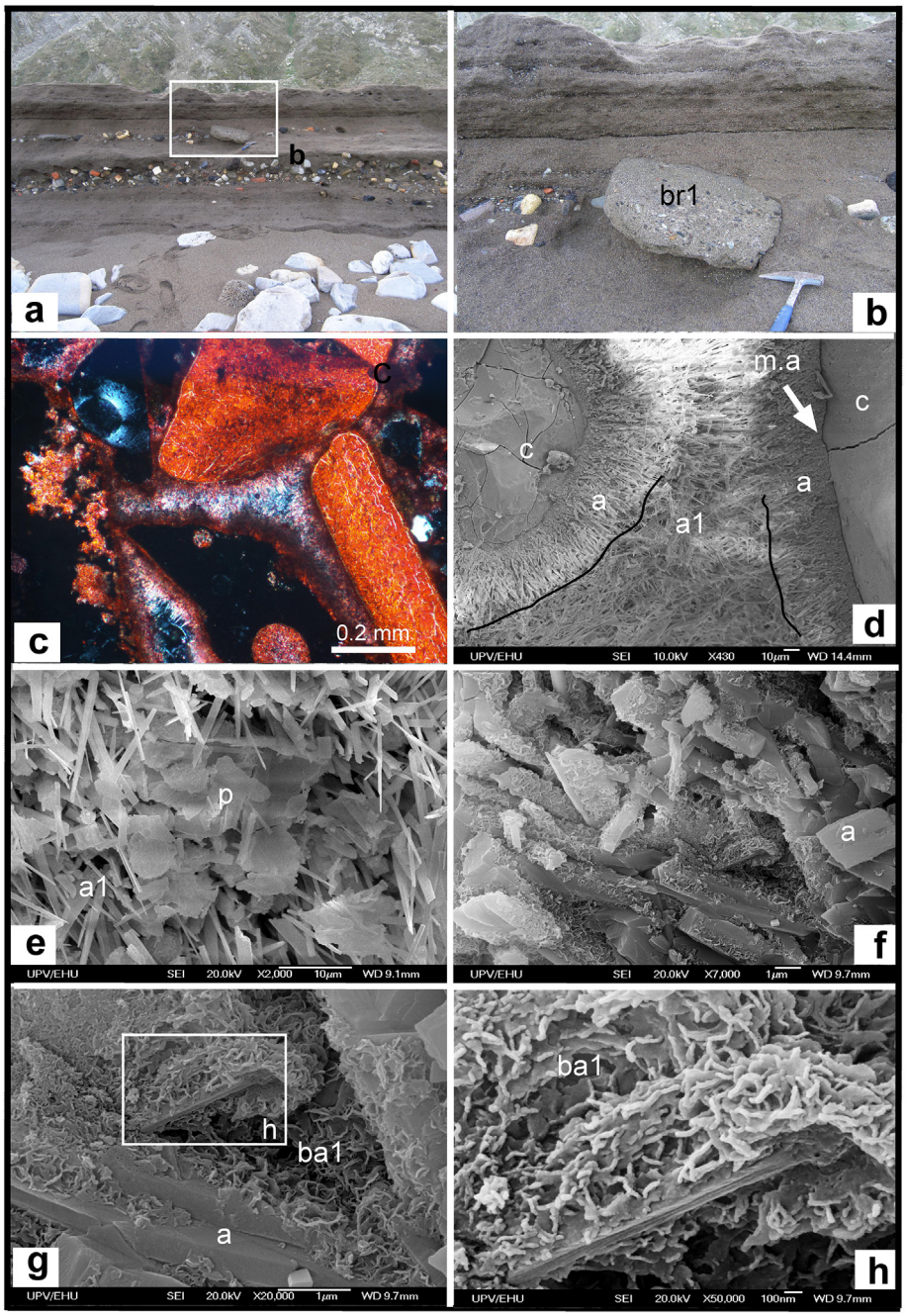

Fig. 13. Foreshore zone with a block accumulation in the Gorrondatxe beach (western part). a–b: Front view following the foreshore erosion front with large slag fragments, refractory bricks and turbidite blocks. The inclusion of beachrock blocks (br1) from the upper shoreface zone occurs. c: Microphotograph of part of block (br1) formed by bioclasts and flux slag clasts strongly cemented by a small dark crown of micritization followed initially by circumgranular aragonite crystals and completed by other disordered aragonite crystals; crossed nicols; stained with Alizarin Red S. d: SEM microphotograph with the clasts (c) cemented with a marked difference between the micritic aragonite (m.a), followed by fine circumgranular aragonite crystals (a) and highly disordered aragonite prisms arranged on the latter (a1). e: Calcite plates (p), according to EDX, superimposed on the previous aragonitic prisms (a1). f: Aragonitic prisms (a) from the first cementation, which are being corroded by *Bacillus*-type activity (ba1). g–h: Details of this *Bacillus*-type activity (ba1) on the rest of the corroded aragonite prisms. (For interpretation of the references to colour in this figure legend, the reader is referred to the web version of this article.)

Another distinctive feature in the foreshore sands (Spl facies), especially in the lower part, close to the upper shoreface, is the general appearance of the lamination (Fig. 3e). Apparently, it is a low-angle, slightly concave and tangential lamination, which looks more "regular", with lateral, systematic differences in grain size, tending to be more parallel and planar as the point of view changes from lateral (Fig. 3e) to more frontal (Fig. 4).

The lamination consists of couplets of coarser-grained and finer-grained laminae (Fig. 3e). These couplets seem to represent two separate modes of sorting among the laminae, since the fine and coarse fractions are found in different laminae, with a separation of different grain sizes in distinct laminae. The thickness of single lamina ranges from 5 to 20 mm. A pair of laminae ranges up to 40 mm in thickness, which is in the upper values for lamination given the average thicknesses (30 ± 10 mm; Reesink and Bridge, 2009).

The basal, coarse-grained lamina in a couplet is erosionally based, which enhances the striping pattern of the lamination. The lamination thickness along the outcrops is not constant and homogeneous. Coarse-grained laminae rest sharply over a basal, slightly erosive surface. Locally, the coarsest granules accumulate at the base of the

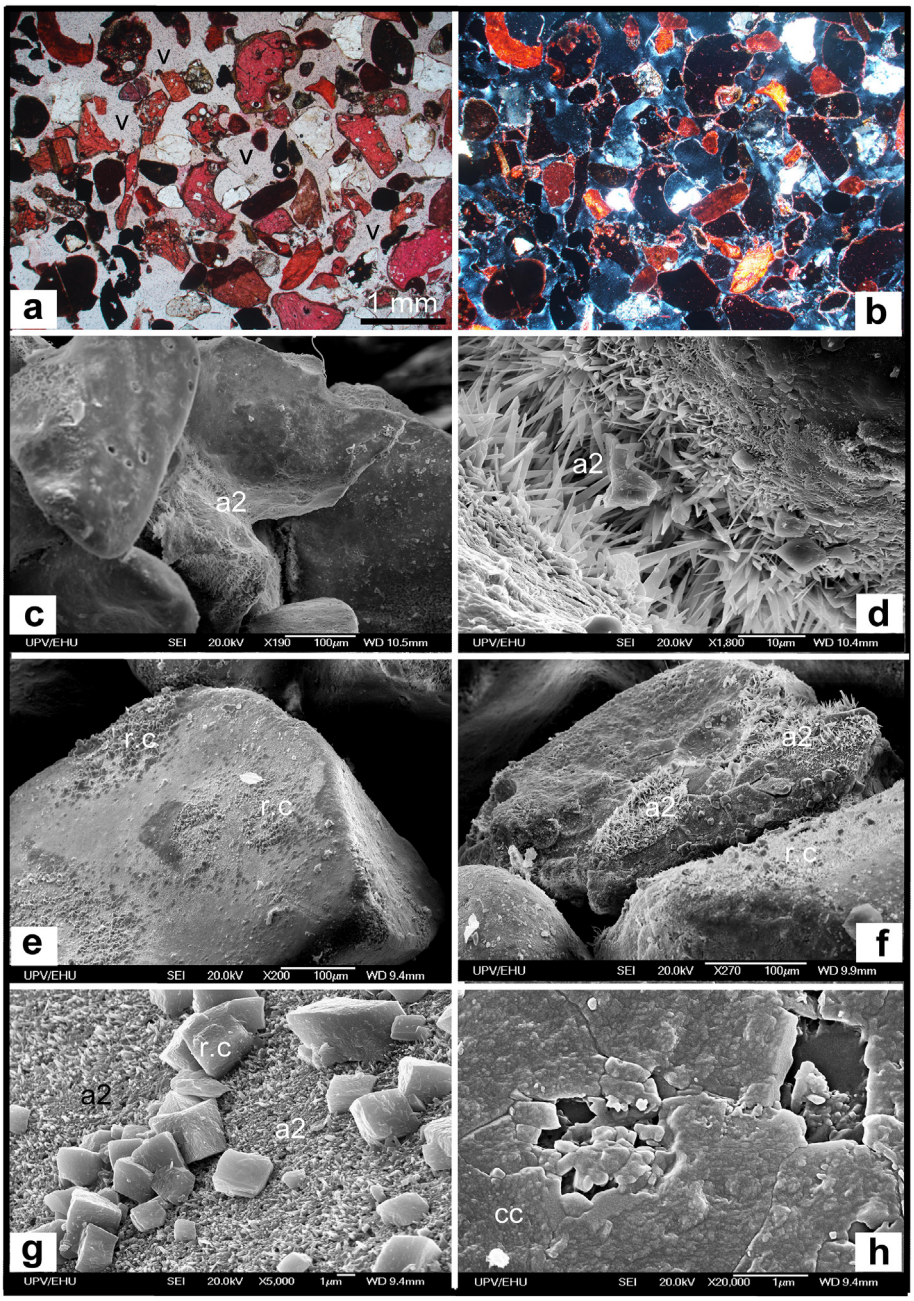

Fig. 14. Gorrondatxe beach backshore (washover). a–b: General appearance with clasts of the same nature as the above-described ones, with extraordinary porosity (v) and very little cementation; stained with Alizarin Red S; parallel and crossed nicols. c–e: Clasts with hardly any meniscus cementation, limited to the contact areas among grains. The small aragonite prisms are intercrossed (a2). f–g: Over short distances there are well-formed rhombohedral calcite aggregates (r.c). The presence of these two polymorphs indicates that the sediment undergoes alternating stages where marine and/or meteoric waters predominate. h: View of the presence of *Coccus*-type nanospheres (cc), indicating that there is also bacterial activity in the washover zone. (For interpretation of the references to colour in this figure legend, the reader is referred to the web version of this article.)

coarse-grained laminae (Fig. 3e), and within these laminae the sediment is often sorted vertically. The finer-grained lamina in a couplet is massive. The lower, coarse-grained in the couplet was probably deposited by grainflow, and the upper, finer-grained lamina reflects subsequent deposition by grainfall (e.g. Passalia et al., 2016). This alternation also suggests that the sediment was delivered in pulses (Kleinhans, 2004).

The origin and development of this kind of lamination is often related with grain-size sorting due to the presence either of superimposed bedforms or flow unsteadiness (Reesink and Bridge, 2007, 2009; Kleinhans, 2004). In this case, as there are no superimposed bedforms, the lamination is considered to have been produced by flow unsteadiness. The grain size of the bedload is expected to decrease as the flow stage decreases (Kleinhans, 2001; Bridge, 2003); thus, the coarser sediments are sedimented at the high-flow stage, and the finer ones at low-flow stages (Bridge, 2003; Kleinhans, 2004). These changes reflect flow unsteadiness linked with cyclical variations in discharge, such as those caused by tides or storms. The variations in current speed that take place either in tidal environments or with the occurrence of a storm may be organized as systematic variations in the grain size of contiguous laminae, with medium to coarse sand sedimented by the stronger currents (at maximum tidal strength or in the storm pulse) and finer sand sedimented by the slower currents (at minimum tidal strength or as the storm recedes).

Although an in-depth discussion of the subenvironment boundaries is beyond the scope of this paper, some observations are worth making.

In this paper, we follow the division of the beach proposed in Dashtgard et al. (2009) and Dashtgard et al. (2021), including the breaker and surf zones in the upper shoreface, an area that can be partially exposed during the lower parts of the tidal cycles. The upper shoreface is preferred for the lower part of the currently exposed beach due to its topography and the sediments and sedimentary structures present in this zone. Observations on the beachrock along the Gorrondatxe beach are restricted to those parts above the low-tide level, and along the exposed beach there is a gradation in grain sizes and sedimentary structures from the low-tide level to the high-tide level and beyond in the backshore area. The upper part of the shoreface and the lower part of the foreshore share some common features. However, the topography, sediment sizes and cementation of the are different from those of the foreshore, and are used here to distinguish the two zones (see above).

The boundary between what is here considered the upper shoreface and the lower part of the foreshore is thus a clear breakpoint step (plunge step), but this step is not necessarily related to the low-water level, but to the breaker zone, which can be located at the upper shoreface (e.g. Dashtgard et al., 2021). In the current beach there is a change in slope between the upper shoreface, where gravels accumulate, and the foreshore, where seaward laminated sands predominate. At the foreshore-backshore boundary, there is another change in slope, in this case related to the mean high-tide water level and a change from the seaward laminated sands of the foreshore to the horizontal laminated sands of the backshore.

5.2. Beach structure and sedimentary evolution

Gorrondatxe shows similarities and differences with respect to other nearby beaches, where the sedimentological features should be similar given their location and exposure to tides and waves (Fig. 1). The beaches to the west (e.g. Tunelboka and Arrigunaga) show a similar development of beachrock. However, they do not shed any further light on the sedimentary evolution of this part of the Basque coast. By contrast, there are major differences between Gorrondatxe (Fig. 15a) and the other nearby beaches to the east (the three beaches closest to Gorrondatxe eastwards are Barinatxe, Sopelana and Barrika from west to east; Fig. 15b to d respectively).

The major differences are the presence of a beachrock in Gorrondatxe and its absence in the other beaches, as well as the particular structure of the beach, especially the slopes and lengths of the subtidal, intertidal and supratidal zones. Moreover, the other beaches are ridge and runnel dissipative beach systems, lacking backshore except in Barinatxe, where a short area, strongly modified by human impact, is located at the toe of the cliffs. The length of the surf zone common to the three other beaches lying eastwards contrasts strongly with Gorrondatxe (Fig. 15a). The surf and breaking areas are longer, ranging from 180 to >250 m (Fig. 15b to d), with a low depositional slope (2–3°). By contrast, at Gorrondatxe the surf and breaking zones are narrow, little >50 m, about a third of the length, and with a high slope in this area (up to 7°). Another difference is the extension of the backshore areas above the mean high-tide water level. The backshore is longer (along the entire beach) and wider (about 100 m) in Gorrondatxe, with vegetated aeolian sands and ponds near the cliffs. By contrast, it is shorter (restricted to some parts of the beach) and narrower (with a maximum width of 50 m) at Barinatxe, lacking ponds, and it is completely absent at Sopelana and Barrika, where almost the entire length of the coast is covered with water at the highest tides. Furthermore, no aeolian sediments are in evidence in the other beaches.

Regarding the evolution of the beach over time, aerial photographs show that this pattern has been constant since the 1950s. The oldest aerial photograph, dating back to 1956, shows that the beach exposed at the low-tide level is coincident with the surf zone both in Gorrondatxe and Barinatxe; a comparison of the aerial images from 1956 and 2020 at low tide shows a similar maximum extension of the sands in the foreshore. During these times the other beaches remained stable. Gorrondatxe, however, shows important changes with time (Fig. 16). In the 1956 image (Fig. 16a), Gorrondatxe seems to be stable, with no erosion taking place on this beach, as shown by the absence of any

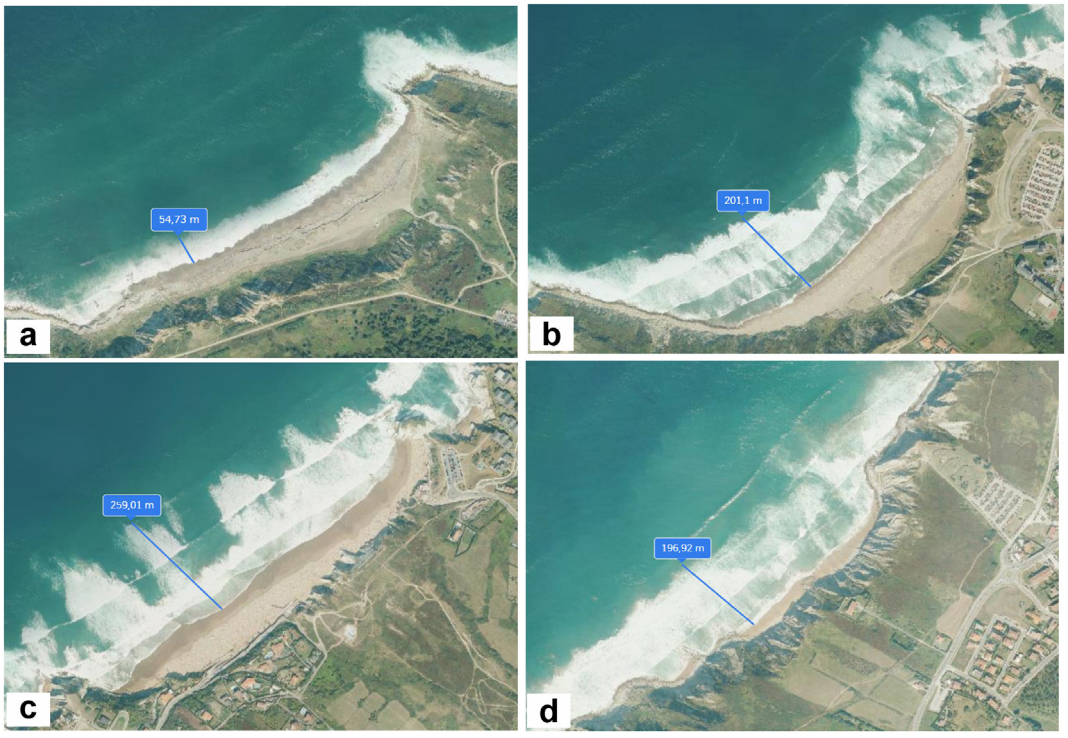

Fig. 15. Views of the studied beach and other nearby beaches for comparison of the length of the shoaling, surf and breaker zones: a: Gorrondatxe beach, a non-barred, reflective beach with a steep-slope shoreface and short surf zone (55 m); b: Barinatxe beach, the closest beach to the NE; c: Sopelana beach; d: Barrika beach. Barinatxe, Sopelana and Barrika are barred, dissipative beaches with longer surf zones (all about 200 m or more). All images are taken at the same scale. Source http://www.ign.es/iberpix2/visor/. (For interpretation of the references to colour in this figure legend, the reader is referred to the web version of this article.)

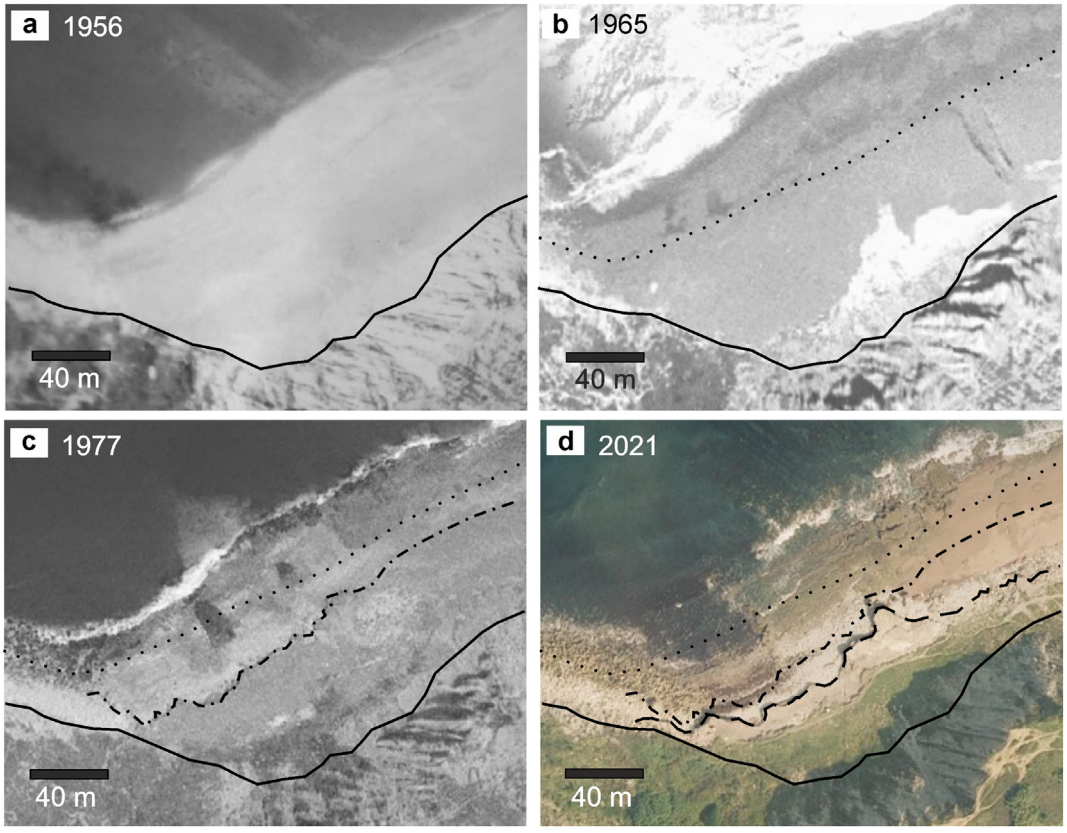

Fig. 16. The western end of the Gorrondatxe beach at various times in the 20th and 21st centuries. a: 1956, the beach is in a stable sedimentary condition, and beachrock is under development; human industrial slag discharges are active; loose sand is the main sediment at the beach surface at this year. The continuous line indicates the base of the cliffs and is kept in the other images for reference. b: 1965, The beach still remained stable and undisturbed except for a human-made trench excavated along the backshore (right), the "Mari Feli mining concession" in search for the metallic ores contained in the beachrock. The whitish areas in the image represent sand removal for the same purposes. The dotted line marks the foreshore-backshore boundary. c: 1977, by this time human industrial slag discharges ended some years ago (Fig. 18); a clear erosive cliff has developed between the foreshore and the backshore (dashes and dots line), which is being actively eroded; gravels and sands are the main sediments. d: 2021, backshore erosive processes are continuously active on the beach, and foreshore-backshore recession is clear (dashed line); gravels are the main sediment on the beach. An average recession rate of about 55 m in 56 years (1965–2021) can be considered (about 1 m/year.) (Orthophotos source: https://www.geo.euskadi.eus/webgeo00-bisorea/es/x72aGeoeuskadiWAR/index.jsp). (For interpretation of the references to colour in this figure legend, the reader is referred to the web version of this article.)

erosive structure or of an erosive cliff along the beach in this image; the beachrock must be under active development below a thin veneer of loose sand. Similarly, in the 1965 image (Fig. 16b) the beach remained undisturbed except for a trench excavated in the backshore area in search for the metallic ores contained in the beachrock ("Mari Feli mining concession") and the removal of surficial sands at the toe of the cliffs (whitish areas in the image) for the same purpose. Nevertheless, in the 1977 image (Fig. 16c) the development of an erosive cliff at the foreshore-backshore boundary, which did not exist previously, is clearly shown along this part of the beach. Since then, this cliff has been actively eroded and retreating, as can be seen in the image from 2021 (Fig. 16d). The current mean high-tide water level is located on this cliff. The storm high-water level can even surpass this cliff, and from this point of view it can be considered the berm of the beach. A comparison of the starting point in 1965 (Fig. 16b) and the most recent view from 2021 (Fig. 16d) clearly shows the foreshore-backshore boundary recession (Fig. 16 b, c and d) in the beach. Although the rates of recession are different in several areas of the beach and over time, a general average rate of about 55 m in 56 years (1965–2021) can be considered; that is a recession average rate of approximately 1 m/year.

These differences are interpreted as being due to the presence of the human-derived sediments, which have caused aggradation on the beach and beachrock development at Gorrondatxe, i.e. a result of the sediments deposited in the sea off the beach over the course of the 20th century (Fig. 17). This was unlike the other eastern beaches, which were not reached by the man-made sediments and thus maintained their original ridge and runnel structure, and similar to the western beaches, where a beachrock also developed.

It is supposed, therefore, that the previous, original stage at Gorrondatxe (pre-20th century) was that of a dissipative, ridge and runnel beach, like the other nearby beaches to the east (Fig. 17a). This is also suggested by a study of benthic foraminifera in borehole cores along this beach (Martínez García et al., 2013). Three different foraminiferal associations have been found: the deepest assemblage represents natural, open beach sediments clearly deposited prior to the slag discharges. The overlying assemblage represents an anthropized beach. The upper assemblage, from the topmost part of the cores obtained in the backshore, suggests a reduced tidal influence, culminating in a presumably aeolian accumulation of littoral foraminifers (Martínez García et al., 2013).

Later, at the onset of the 20th century, huge amounts of man-made debris started to be deposited on the sea bottom off Gorrondatxe (and other western areas of the coast) (Fig. 18). These debris were composed of sands, gravel and slag, and its deposition continued throughout the century, in an area that was hitherto more or less stable, giving rise to a major change in the sedimentary conditions. Once deposited, these sands, gravels and slag produced a large submarine sediment bank. Much of the sediment was subsequently moved and accreted onto Gorrondatxe, but not the other eastern beaches, resulting in a major change from a dissipative to a reflective beach (Fig. 17a–b). Coastal accretion and aggradation took place due to the onshore migration of the bank, which was welded onto the coast, serving as an important subtidal sand reservoir for the beach (Fig. 17b).

This change involved a change in foraminiferal assemblages from those characteristic of a natural, open beach to an anthropized beach (Martínez García et al., 2013), and also sedimentary adjustments in the different beach zones. Thus, the foreshore zone is generally steeper than in the

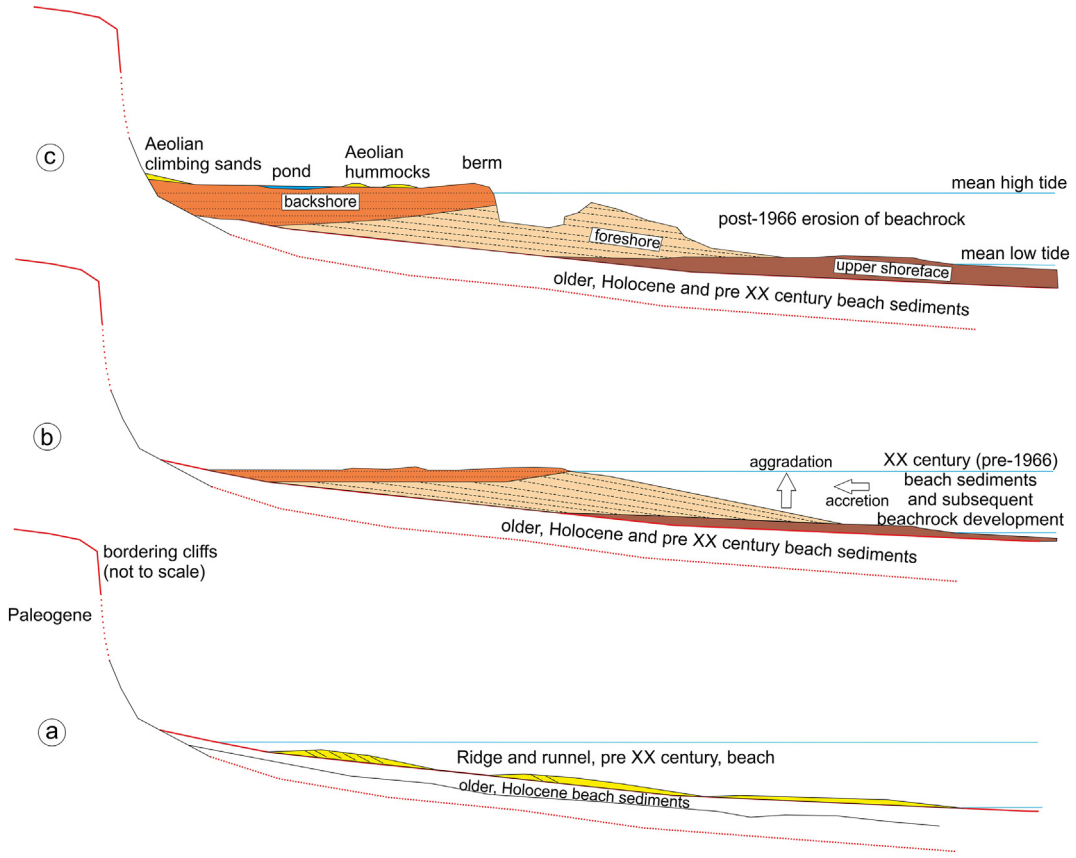

Fig. 17. Evolutionary model for the Gorrondatxe beach over time (19th to 21st centuries). a: pre-20th-century beach based on other nearby beaches (see Fig. 15); the Gorrondatxe beach was probably a ridge and runnel dissipative beach. The presence of a natural association of open-beach benthic foraminifera is characteristic of these sands (Martínez García et al., 2013). b: 20th-century beach (pre-1966); the huge discharge of anthropic deposits and slag in open waters off the beach resulted in a change in the slope of the beach, the accretion and aggradation of part of these anthropic sediments, and the subsequent and progressive cementation of the beach sediments, below the surface; as they were constantly buried by new fresh, anthropic sediments, with the development of beachrock. The benthic foraminiferal association changes to an association dominated by an anthropized assemblage (Martínez García et al., 2013). c: current state of the beach (post-1966), the beach and beachrock are under active erosion, causing a return to the previous state. (For interpretation of the references to colour in this figure legend, the reader is referred to the web version of this article.)

other eastern beaches (Figs. 15 and 17b), and shows a change in slope both seaward, to the upper shoreface, with the development of a low-tide terrace and plunge step (with the maximum grain size of the beach), and landwards, to the backshore, with the development of a relatively flat surface where active aeolian winnowing of sands is common, also allowing the development of small ponds on this surface (Fig. 17b–c). Notwithstanding the important accretion of sand onto the beach over the first part of the 20th century (pre-1966; Fig. 17b), the main change in the beach was the beachrock development as a self-sustained process due to the subsequent and progressive cementation, below the surface, of the loose beach sediments as they were constantly buried by new fresh, anthropic sediments. (Fig. 17b), which is clearly related to the presence of these sediments (Figs. 16–18) since the eastern beaches lack beachrocks.

While the human source of sediment remained stable and more or less constant throughout the first half of the 20th century, the new reflective profile and beachrock development were also stable, suggesting that these sedimentary inputs were rapidly recycled to the beachface. When the human discharges ended in 1966, the sourcing of sediment and slag to the beach was cut off. As a result, the equilibrium of erosion and sedimentation changed to favour erosive processes, which started to predominate both in this part and the rest of the beach (Figs. 16c–d and 17c),

The location of beachrock sediments within the current beach also suggests two further points. Firstly, the overall sedimentary system remained more or less stationary during the development of the beachrock (Fig. 17b), while the sources of sediment were active (until 1966; Fig. 18). Beachrock and current beachface zones are found in almost exactly the same relative location on the beach and nearby cliffs. Secondly, this location clearly suggests a rapid, vertical aggradation and a progradation during the beachrock development (Fig. 17b). Aggradation and progradation are suggested by the presence of foreshore facies on top of the upper shoreface facies (Fig. 4). Washover deposits were produced when storm surges overtopped the foreshore sediments, creating sheet deposits that extended into the backshore (Fig. 17b). With time, these washover processes increased the width of the backshore, providing environments favourable to the stabilization of aeolian sediments (Fig. 17b–c), as seen in the present beach (Figs. 15a and 16d).

Several phases of cementation and beachrock development are clearly indicated by the presence of large beachrock fragments in the form of clasts within any beach zones (upper shoreface, foreshore and backshore). The beachrock was eroded, then resedimented within loose sands and gravels, and cemented again. Along the best-exposed section of the beachrock (Figs. 2e, 4, and 13a–b), there are three superposed beds with beachrock clasts, which is consistent with the presence of several major erosive surfaces along the exposed cliffs (Fig. 4). The beds with beachrock clasts are beds 7a-7b (with a large erosive surface at the base), beds 13–14-14b (erosive surface) and beds 17-18-18b (erosive surface) (Fig. 4). Each of these beds also shows an increase in grain size, with the presence of gravels at the base.

The causes and origins of these several phases are not well understood. They are clearly visible due to the presence of beachrock clasts embedded in newly formed beachrock. Beachrock clasts are also related to erosive surfaces. A major sedimentary change thus occurred, either in the energy of the processes or in the source of sediments. Large storms affect this coast yearly, but this probably causes what can be considered the "normal" lamination discussed in Section 5.1. There are no records of extreme events in the course of the 20th century; such extreme events can

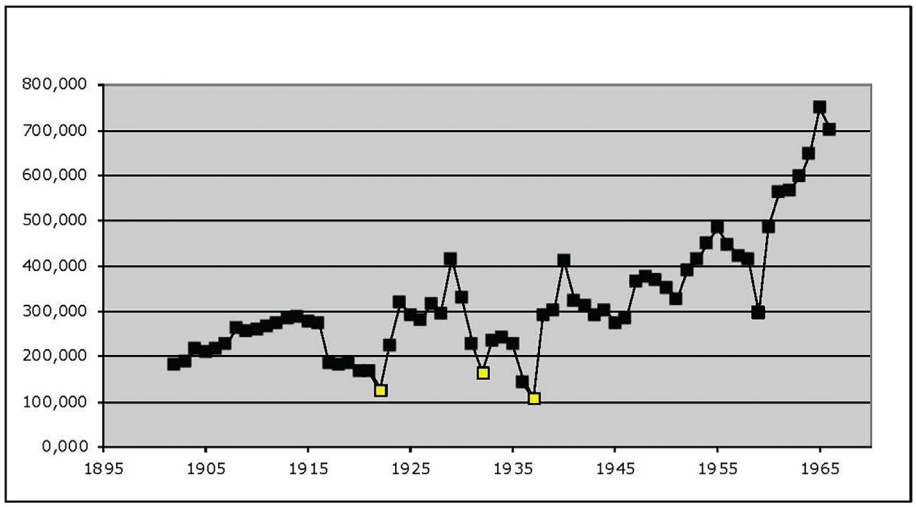

Pig Iron produced by "Altos Hornos de Vizcaya" during 1902 to 1966 (tons)

Years	tms	Years	tms	Years	tms	Years	tms
1902	182,552	1921	167,831	1940	410,979	1959	296,642
1903	189,803	1922	124,968	1941	322,437	1960	484,900
1904	215,230	1923	224,300	1942	311,405	1961	562,434
1905	209,319	1924	320,535	1943	290,561	1962	566,378
1906	216,005	1925	290,234	1944	301,449	1963	597,354
1907	226,194	1926	279,352	1945	274,107	1964	647,904
1908	262,151	1927	315,506	1946	281,991	1965	748,346
1909	255,699	1928	295,403	1947	363,283	1966	700,666
1910	257,886	1929	415,135	1948	374,741		
1911	265,900	1930	330,177	1949	368,671	**Pig Iron**	
1912	274,087	1931	227,367	1950	351,494	TOTAL	20.698,323
1913	284,891	1932	165,273	1951	326,157		
1914	286,078	1933	232,877	1952	388,710		
1915	275,737	1934	240,467	1953	413,222	**Slag**	
1916	274,308	1935	225,920	1954	450,768	TOTAL from	6.209,497
1917	186,423	1936	144,109	1955	484,373	to	12.418,994
1918	182,812	1937	106,802	1956	447,671		
1919	184,340	1938	292,102	1957	421,533		
1920	167,652	1939	301,946	1958	412,776		

Fig. 18. "Pig Iron" produced by the "Altos Hornos de Vizcaya" from 1902 to 1966 (tons). There is a general trend toward an increase in production over time, with two important minimums in 1917–1922 (related to the end of the 1st World War) and in 1931–1937 (a major period of political change in Spain, including the start of the Spanish Civil War). These decreases in production resulted in a lower contribution of anthropic sediments to the beaches and in beach and beachrock erosion. Large, eroded blocks of beachrock were then included within newly formed loose sediments and cemented again later. Each ton of pig iron generates 300–600 kg of slag (Apraiz, 1978, p. 351), which produces a final amount of approximately 6–12 million tons. (For interpretation of the references to colour in this figure legend, the reader is referred to the web version of this article.)

thus only remain a possibility for beachrock erosion and resedimentation of large beachrock clasts. Another cause could be the lack of newly produced human sediments on the marine bank, later to be sourced to the beach (mainly sand-sized sediments). Currently, it is interpreted here that the absence of sediments from 1966 onwards caused a change in the state of the beach from active sedimentation (pre-1966, Fig. 16a–b) to active erosion (post-1966, Fig. 16c–d). Such a pattern might have occurred in the 20th century related to the decrease in human-derived sediments. There are two major periods of sediment depletion in the curve of sedimentary supply (1917–1922 and 1931–1937; Fig. 18). The periods where sediments were only partially available to the beach can be presumed to have caused the occurrence of major sedimentary erosive events, and the new arrival of fresh and loose sediments to have caused sediment reactivation; since many active beachrock form in a matter of less than a year (Frankel, 1968; Friedman, 2011; Wiles et al., 2018).

5.3. Beachrock: its origin and development

Beachrock can be produced by four cementation routes, which may be complementary: 1) the physicochemical precipitation of a high Mg-calcite content and aragonite from seawater as a result of high temperatures, $CaCO_3$ supersaturation and/or evaporation; 2) the physicochemical precipitation of a low Mg calcite content and aragonite, by mixing meteoric water and fresh groundwater with seawater; 3) the physicochemical precipitation of a high Mg-calcite content and aragonite by CO_2 degassing of water from the pores of the beach sediment; 4) the precipitation of micritic calcium carbonate as a by-product of microbiological activity (Krumbein, 1979; Turner, 2005; Vousdoukas et al., 2007 and references herein; see also Khadkikar and Rajshekkar, 2003; Erginal et al., 2008).

Modern beachrocks are generally restricted to warm climatic belts between latitudes 35°N and 35°S (Friedman, 2011). In temperate latitudes, seawater is slightly undersaturated in $CaCO_3$, and the presence of beachrocks is thus rarely recorded in the literature. However, the contribution of carbonate-enriched meteoric waters seems to trigger cementation in calcite with a low Mg content (Rey et al., 2004). Initially, in a water-mixing zone, the higher the temperature reached, the lower the percentage of seawater required to achieve the supersaturation and precipitation of carbonate cement (Mauz et al., 2015).

In this case, the main cementation, with well-developed, drusy, circumgranular aragonite surrounding all the clasts in the upper shoreface, is characteristic of a marine phreatic zone, even though it has not completely filled all the pores, being typical of a saturated marine environment. Prior to the growth of this cement, very fine micritic aragonite lamellae were arranged in contact with clast surfaces, showing irregular boundaries with the better-developed, later aragonite crystals (Fig. 9e). One or both of these types are what were recognized in previous studies of the area (Knox, 1973; Aizpiri, 1983; García-Garmilla, 1990; Iturregui et al., 2014; Arrieta et al., 2011, 2017).

However, these earlier papers lack any recognition of the presence of bacterial activity in the origin and development of the beachrock. Thus, the triggering, biologically induced carbonated precipitation in the beachrock seems to be related to metabolic, ureolytic bacterial activity, such as that of *Myxococcus xanthus* or other smaller bacteria such as *Brevundimonas diminuta*, whose presence is suggested at high magnifications (Fig. 9g–h).

It should be borne in mind that during the years when the beachrock was being formed (1902–1966), all the domestic and industrial wastewater was being discharged into the Bilbao estuary without undergoing any water treatment. It was only from 1979 that the "Integral Sanitation Plan of Metropolitan Bilbao" (*Plan Integral de Saneamiento de Bilbao Metropolitano*) was approved by the city council, and from 1990 that the "Galindo water treatment plant" started working, and the sewage of 850,000 people was treated and purified (about 350,000,000 l a day; https://culturacientifica.com, 2020/06/01).

Without the need for light, therefore, the metabolic activity of the bacteria present in the sediment triggered a significant rise in pH during the hydrolyzation of the urea, due to the emission of NH_3 and CO_2, with the transformation of NH_3 to NH_4^+ and the formation of OH^-. This promoted carbonate supersaturation and calcification around the bacteria, as experimentally demonstrated by Rodríguez-Navarro et al. (2003) and Rodríguez-Navarro et al. (2007) and confirmed by other authors (Neumeier, 1998, 1999; Dhami et al., 2013; Ge et al., 2021).

$$NH_{3\ (g)} + H_2O \leftrightarrow NH_{4(aq)}{}^{+} + OH_{(aq)}{}^{-}.$$

The increase in pH allowed a subsequent rise in the concentration of $CO_{3(aq)}^{2-}$ in cultures according to:

$$CO_{2\ (g)} + H_2O_{(l)} \leftrightarrow H_2CO_{3(aq)} \leftrightarrow HCO_{3\ (aq)}{}^{-} + H_{(aq)}{}^{+} \leftrightarrow CO_{3(aq)}{}^{2-} + 2H_{(aq)}{}^{+}.$$

In the presence of $Ca_{(aq)}$, some areas might have reached supersaturation with respect to a carbonate phase (aragonite, vaterite, calcite), resulting in precipitation following the equilibrium formula:

$$CO_{3(aq)}{}^{2-} + Ca_{(aq)}{}^{2+} \leftrightarrow CaCO_{3(s)}.$$

The source of Ca in temperate latitudes may be both marine and meteoric waters, in our case with an additional supply from the presence of Ca and Mg silicate slags (pseudowollastonite and gehlenite-akermanite) in the sediment, derived from the limestone-dolomites used as fluxes in blast furnaces.

Moreover, the bacteria commonly recognized in karst caves (Altamira, Tito Bustillo, Candamo in Spain; Grotta dei Cervi in Italy), in the catacombs of Malta, and with volcanic substrates (Saint Callixtus Catacombs, Rome, Italy) are usually covered and fossilized by hydromagnesite $Mg_5(CO_3)_4(OH)_2 \cdot 4H_2O$ and calcium carbonate polymorphs such as vaterite and aragonite (Cañaveras et al., 1999; Groth et al., 2001; Sánchez-Moral et al., 2003; Cuezva et al., 2009; Zammit et al., 2011).

Even so, microbially induced calcium carbonate precipitation via urea hydrolysis is the simplest and most widely used method for the precipitation of carbonates in several technical applications pertaining to the durability of buildings, remediation of the environment, and the sequestration of atmospheric CO_2 filler material in rubbers and plastics (Dhami et al., 2013; Bibi et al., 2018).

In the foreshore zone of Gorrondatxe, the different facies are cemented by fibrous-radial aragonite (c1), with their intercrossing needles indicating that the environmental conditions have changed with respect to the upper shoreface zone, although it seems that sea waters are still predominant, with a smaller contribution of meteoric waters in a vadose environment (Figs. 9; 11). However, the contribution of the meteoric waters has enough influence to change the habit of the aragonite. The presence of diatom frustules and coccoliths provides further evidence of the activity and supply of marine waters (Fig. 10f, h).

The predominance of dark tones in these facies is occasionally modified by lighter-toned laminations. In these clearer laminations, there is a meniscus cementation of radially shaped aragonite crystals mixed with smaller bladed calcite crystals. This suggests that these areas received an occasional, but locally important, contribution of seawater, which was sufficiently retained between the layers to generate a different cementation than usual. The loci of nucleation, from which the growth of the radial aragonite prisms started, correspond to a set of nanospheres of bacterial origin, fossilized by a carbonate patina in the form of a clotted micrite (Fig. 12e–g).

Likewise, the beachrock blocks (br1) belonging to the upper shoreface that have been eroded and included in the foreshore (Fig. 13a–b) show a more complete diagenetic behaviour over time. The new environmental conditions have maintained the previous aragonite cements (a), and have precipitated, in favourable empty spaces, intercrossed aragonite needles (a1) as well as irregular calcite plates (p) (Fig. 13c–e). Local episodes of corrosion with intense bacterial activity (ba1), albeit with different, rod-shaped bacterial cells from those found in the upper foreshore facies, are also noticeable (Fig. 13f–h). This indicates the strong sensitivity and rapid response of the cements to slight changes in the proportion of marine versus meteoric waters when passing from one beach zone to another.

The simplest explanation for the dissolution of a carbonate cement without bacterial intervention is contact with $CaCO_3$-undersaturated waters. All marine, hypersaline and slightly brackish waters are saturated with respect to aragonite; dissolution always results from the action of fresh water incorporated in a meteoric vadose environment (Neumeier, 1998; p. 47). This seems to occur in these eroded blocks (br1, Fig. 13), but the bacterial presence leads us to suggest that the bacteria generated a drop in pH with a greater contribution of H^+ (Konhauser, 2007).

In the supratidal (washover) sediments of the backshore, with hardly any compaction, a very weak cementation occurs in a vadose environment with a spongy appearance, which easily breaks down by mere hand pressure. The clasts are cemented in meniscus, both by acicular aragonite crystals and by rhombohedral calcite crystals, which indicates a mixture of waters conditioned by the successive minor contributions of marine waters in a supratidal environment with a predominance of meteoric waters. Depending on whether it occurred in times of storms or of heavy rains, the washover deposits acted as an open aquifer, favourable to the development of weak cementation (Fig. 14c–g). The presence of *Coccus*-type bacteria fossilized in the washover sediments of the backshore indicates that metabolic activity also had a clear impact on the cementation of the sediments in this zone (Fig. 14h).

6. Conclusions

Data and sedimentary structures alike suggest that Gorrondatxe is a wave-dominated, mesotidal coastal system and beach. It can be considered an example of a tidally-modulated shoreface (Dashtgard et al., 2021), with a clear storm influence evidenced by the presence of high-turbulence facies and large erosive surfaces probably related to beach cusp development.

Lithology, bedding and sedimentary structures, and their location in relation to the current beach reveal upper shoreface, foreshore and

backshore zones within the beachface. The upper shoreface is located around the low-water level and contains the coarsest grain sizes (gravels and coarse sands with multidirectional trough and planar cross-stratification). The foreshore is located in the main intertidal zone, being composed mainly of sands with minor gravels. A distinctive low-angle, seaward-dipping, planar-parallel lamination resulting from swash and backwash wave action is the main facies. Large erosive surfaces and channels have also been recognized at the foreshore, the former representing major sedimentary breaks and the latter the development of scarce incised channels. The backshore is an area with a mixture of marine sands (washover) and non-marine sands and muds (aeolian, subaerial ponds) in a topographically higher position, above the high-tide water level.

The beach contains a mixture of sand- and gravel-sized sediments. Of the different types of mixed sand/gravel beaches, it can be considered an extreme example of a composite beach (Jennings and Shulmeister, 2002). The facies model represents a fining-upward aggradational and progradational beach in which the upper shoreface contains the coarsest grain sizes, being dominated by gravels; coarse to fine-grained sands and minor gravels occupy the foreshore; and medium to fine-grained sands with rare layers of gravel predominate at the backshore.

The development of the beachrock is related to blast furnace waste disposal (Altos Hornos de Vizcaya) off the coast of Bilbao from the beginning of the 20th century. Over the following decades, a large amount of waste was deposited, creating a submarine bank that later became attached to the coast and probably triggered the onset of beachrock cementation. Eventually, this waste deposit altered the coast so much that no natural shoreline existed in several places.

Our sedimentological study of the beachrock has further allowed the beachrock itself to be characterized and provided important information regarding the facies relationships and the organization of the modern sediments on the beach. Visual observations of the beachrock along a transect from the upper shoreface to the backshore clearly indicate that there are different cements, grain sizes, and degrees of lithification of the beachrock across the different zones of this transect, suggesting that the beachrock-related processes, though coetaneous, were not the same in all these zones and that different cements developed at the same time. This raises the question of whether previously described differences in the origin and interpretation of the beachrock could be related to wider sedimentological aspects of beaches rather than specific aspects of the beachrock.

There are major differences in the facies cementation of the sands within these three zones, which can be used as a tool for recognizing these facies in the stratigraphic record or in well cores when other kinds of data are not available. The sandstones at the upper shoreface are hard and well-cemented, with a whitish circumgranular aragonite cement and good intergranular porosity. The sands at the foreshore are medium-hard, with an irregular aragonite needle cement, and show a higher intergranular porosity. The sands at the backshore are slightly cemented with brown irregular aragonite and rhombohedral calcite aggregates, and show the highest intergranular porosity.

On the origin of cements, firstly, SEM images showing the presence of *Coccus*-type bacteria (cc) in all the different facies and zones of the beach are the best proof of metabolic activity, probably of ureolytic bacteria, in the origin of all these cements. During the hydrolyzation of urea, there is a significant rise in pH due to the emission of NH_3 and CO_2 with the transformation of NH_3 to NH_4^+ and the formation of OH^-, which favours carbonate supersaturation. On the other hand, most of the precipitation of the aragonitic cement, with different habits (a; a1; a1*), is triggered by changes in the percentage of dominant seawater versus meteoric water. These changes are even capable of redirecting a second, differentiated cementation in the previously cemented beachrock blocks (br1) when they are eroded and dragged to the foreshore. When the cementation occurs in a backshore environment (washover facies), small aragonite prisms (a2) are also visible, but the difference is evident with the incorporation of well-developed rhombohedral calcite aggregates (r.c), indicative of the important presence of meteoric waters.

Over the course of the 20th century, Gorrondatxe evolved from a formerly dissipative, ridge and runnel beach, like other nearby beaches, to an active, aggrading and prograding, reflective beach and to an inactive beach prone to erosion. The anthropic deposition of huge amounts of man-made debris at the sea bottom off the beach gave rise to a major change in the sedimentary conditions. A large submarine bank developed and later accreted to this beach and other nearby ones, resulting in the change from a dissipative to a reflective beach. Coastal aggradation and progradation took place due to the onshore migration of this bank. While the human source of sediment remained stable and constant throughout the first half of the 20th century, the new reflective profile and the development of the beachrock were also stable, suggesting that these sedimentary inputs were rapidly recycled to the beachface. Another major change occurred when the waste discharges ended in 1966, and the former sediments and beachrock started to be eroded to their current state.

Acknowledgements and funding

The present study has been funded by the Universidad del País Vasco/Euskal Herriko Unibertsitatea (UPV/EHU), research group GIU18/16317/05; MINECO/MCI/ERDF-EU project PID2019-105670GB-I00/AEI/10.13039/501100011033 of the Spanish Government. We sincerely appreciate the information provided by N. Redondo (Basque Country Coastal Demarcation Office). We thank A.H. Molpeceres Atucha (Department of Sustainability and the Natural Environment; Bizkaia Provincial Council), M. Martínez Vítores (Altos Hornos de Vizcaya), and the technicians J. Sanguesa, S. Martínez-Armas, S. Suárez Bilbao, and F. De la Cruz Sgiker (UPV/EHU). Rupert David Victor Glasgow thoroughly revised the English version of the manuscript. The paper has benefited gratefully from the insight and by critical reviews of the Editor (Dr. Massimo Moretti) and two unknown referees.

Data availability

No data was used for the research described in the article.

Declaration of competing interest

The authors declare that they have no known competing financial interests or personal relationships that could have appeared to influence the work reported in this paper.

References

Aizpiri, F., 1983. Cementación por vertidos industriales en playas de Vizcaya. Universidad del País Vasco/Euskal Herriko Unibertsitatea unpublished, 35 p.

Allen, J.L., Johnson, C.L., 2010. Facies control on sandstone composition (and influence of statistical methods on interpretations) in the John Henry Member, Straight Cliffs Formation, Southern Utah, USA. Sedimentary Geology 230, 60–76. https://doi.org/10.1016/j.sedgeo.2010.06.023.

Apraiz, J., 1978. Fabricación de Hierro, Aceros y Fundiciones. Tomo 1. Ediciones Urmo, Bilbao (368 pp.).

Arnott, R.W.C., 1993. Quasi-planar-laminated sandstone beds of the lower cretaceous Bootlegger member, north-central Montana: evidence of combined-flow sedimentation. Journal of Sedimentary Petrology 63, 488–494. https://doi.org/10.1306/D4267B31-2B26-11D7-8648000102C1865D.

Arrieta, N., Goienaga, N., Martínez-Arkarazo, I., Murelaga, X., Baceta, J.I., Sarmiento, A., Madariaga, J.M., 2011. Beachrock formation in temperate coastlines: examples in sand-gravel beaches adjacent to the Nerbioi-Ibaizabal Estuary (Bilbao, Bay of Biscay, North of Spain). Spectrochimica Acta A 80, 55–65. https://doi.org/10.1016/j.scitotenv.2016.12.132.

Arrieta, N., Iturregui, A., Martínez-Arkarazo, I., Murelaga, X., Baceta, J.I., De Diego, A., Olazabal, M.A., Madariaga, J.M., 2017. Characterization of ferruginous cements related with weathering of slag in a temperate anthropogenic beachrock. Science of the Total Environment 581–582, 49–65. https://doi.org/10.1016/j.scitotenv.2016.12.132.

Astibia, H., 2012. Tunelboka y Gorrondatxe (Getxo, Bizkaia), fósiles humanos para el Antropoceno. http://www.euskonews.com/0640zbk/gaia64002es.html.

Bibi, S., Oualha, M., Ashfaq, M.Y., Suleiman, M.T., Zouari, N., 2018. Isolation, differentiation and biodiversity of ureolytic bacteria of Qatari soil and their potential in microbially

induced calcite precipitation (MICP) for soil stabilization. RSC Advances 8, 5854–5863. https://doi.org/10.1039/C7RA12758H.
Binkley, K.L., Wilkinson, B.H., Owen, R.M., 1980. Vadose beachrock cementation along a Southeastern Michigan marl lake. Journal of Sedimentary Petrology 50, 953–962. https://doi.org/10.1306/212F7B30-2B24-11D7-8648000102C1865D.
Blavette, A., O'Sullivan, D.L., Alcorn, R., Lewis, T.W., Egan, M.G., 2014. Impact of a medium-size wave farm on grids of different strength levels. IEEE Transactions on Power Systems 29 (2), 917–923. https://doi.org/10.1109/TPWRS.2013.2284513.
Bridge, J.S., 2003. Rivers and Floodplains: Forms, Processes and Sedimentary Record. Blackwell Publishing, Oxford https://doi.org/10.1306/212F7B30-2B24-11D7-8648000102C1865D (504 pp.).
Cañaveras, J.C., Hoyos, M., Sánchez-Moral, S., Sanz-Rubio, E., Bedoya, J., Soler, V., Groth, I., Schumann, P., Laiz, L., Gonzalez, I., Saiz-Jimenez, C., 1999. Microbial Communities Associated to hydromagnesite and needle-fiber aragonite deposits in a karstic cave (Altamira, Northern Spain). Geomicrobiology Journal 16, 9–25. https://doi.org/10.1080/014904599270712.
Clifton, H.E., 1969. Beach lamination: nature and origin. Marine Geology 7, 553–559. https://doi.org/10.1016/0025-3227(69)90023-1.
Collinson, J.D., Thompson, D.B., 1982. Sedimentary Structures. George Allen & Unwin, London (194 pp.).
Cooke, R.U., Warren, A., Goudie, A.S., 1993. Desert Geomorphology. CRC Press https://doi.org/10.1201/b12557 (534 pp.).
Cuezva, S., Sánchez-Moral, S., Saiz-Jiménez, C., Cañaveras, Juan Carlos, 2009. Microbial communities and associated mineral fabrics in Altamira Cave, Spain. International Journal of Speleology Official Journal of Union Internationale de Spéleologie 38 (1), 83–89. https://doi.org/10.5038/1827-806X.38.1.9.
Dalrymple, R.W., Choi, K.S., 2003. Sediment transport by tides. In: Middleton, G.V. (Ed.), Encyclopedia of Sediments and Sedimentary Rocks. Kluwer Academic Publishers, pp. 606–609.
Dashtgard, S.E., Gingras, M.K., Maceachern, J.A., 2009. Tidally modulated shorefaces. Journal of Sedimentary Research 79, 793–807. https://doi.org/10.2110/jsr.2009.084.
Dashtgard, S.E., Vaucher, R., Yang, B., Dalrymple, R.W., 2021. Wave-dominated to tide-dominated coastal systems: a unifying model for tidal shorefaces and refinement of the coastal-environments classification scheme. Geoscience Canada 48, 5–22. https://doi.org/10.12789/geocanj.2021.48.
Dhami, N.K., Sudhakara Reddy, M., Mukherjee, A., 2013. Biomineralization of calcium carbonates and their engineered applications: a review. Frontiers in Microbiology 4, 314. https://doi.org/10.3389/fmicb.2013.00314.
Dickson, J.A.D., 1965. A modified staining technique for carbonates in thin section. Nature 205, 587. https://doi.org/10.1038/205587a0.
Elorza, J., 2021. Ostende and Arrigunaga beaches, two different interventions and subsequent geomorphological changes in northern Spain: an appropriate policy to follow? Revista de la Sociedad Geológica de España 34 (1), 25–35.
Erginal, A.E., Güneç, N.K., Bozcu, M., Ertek, A., Güngüneş, H., Sungur, A., Türker, G., 2008. On the origin and age of the Arıburnu beachrock, Gelibolu Peninsula, Turkey. Turkish Journal of Earth Sciences 17, 803–819.
Fisher, R.V., 1971. Features of coarse-grained, high concentration fluids and their deposits. Journal of Sedimentary Petrology 41, 916–927. https://doi.org/10.1306/74D723B5-2B21-11D7-8648000102C1865D.
Frankel, E., 1968. Rate of formation of beachrock. Earth and Planetary Science Letters 4, 439–440. https://doi.org/10.1016/0012-821X(68)90020-4.
Friedman, G.M., 2011. Beachrocks record Holocene events, including disasters. Carbonates and Evaporites 26, 97–109. https://doi.org/10.1007/s13146-011-0056-3.
García-Garmilla, F., 1990. Diagénesis de las arenitas: ejemplos del Cretácico, Terciario y Cuaternario de la zona de Bilbao. Kobie (Serie Ciencias Naturales) XIX, 85–103.
Ge, Y., Della Porta, G., Pederson, C.L., Lokier, S.W., Hoffmann, R., Immenhauser, A., 2021. Botryoidal and Spherulitic aragonite in carbonates associated with microbial mats: precipitation or diagenetic replacement product? Frontiers in Earth Science 9, 698952. https://doi.org/10.3389/feart.2021.698952.
Gischler, E., Lomando, A.J., 1997. Holocene cemented beach deposits in Belize. Sedimentary Geology 110 (3–4), 277–297. https://doi.org/10.1016/S0037-0738(96)00088-7.
Groth, I., Schumann, P., Laiz, L., Sánchez-Moral, S., Cañaveras, J.C., Saíz-Jiménez, C., 2001. Geomicrobiological study of the Grotta dei Cervi, Porto Badisco, Italy. Geomicrobiology Journal 18, 241–258. https://doi.org/10.1080/01490450152467778.
Hanor, J.S., 1978. Precipitation of beachrock cements: mixing of marine and meteoric waters vs. CO2-degassing. Journal Sedimentary Petrology 48, 489–501. https://doi.org/10.1306/212F74B4-2B24-11D7-8648000102C1865D.
Hart, B.S., Plint, A.G., 1989. Gravelly shoreface deposits: a comparison of modern and ancient facies sequences. Sedimentology 36, 551–557. https://doi.org/10.1111/j.1365-3091.1989.tb02085.x.
Hart, B.S., Plint, A.G., 1995. Gravelly shoreface and beachface deposits. In: Plint, A.G. (Ed.), Clastic Facies Analysis – a Tribute to the work and teaching of Harold G. Reading. International Association of Sedimentologists, Special Publication22, pp. 75–99.
Hayes, M.O., 1967. Hurricanes as geological agents, south Texas coast. American Association of Petroleum Geologists Bulletin 51, 937–942. https://doi.org/10.1306/5D25C0FF-16C1-11D7-8645000102C1865D.
Hesp, P.A., 1999. The beach backshore and beyond. In: Short, A.D. (Ed.), Handbook of Beach and Shoreface Morphodynamics. Wiley, Chichester, pp. 145–170.
Hiroki, Y., Terasaka, T., 2005. Wavy lamination in a mixed sand and gravel foreshore facies of the Pleistocene Hosoya Sandstone, Aichi, central Japan. Sedimentology 52, 65–75. https://doi.org/10.1111/j.1365-3091.2004.00682.x.
Holland, K.T., Elmore, P.A., 2008. A review of heterogeneous sediments in coastal environments. Earth-Science Reviews 89, 116–134. https://doi.org/10.1016/j.earscirev.2008.03.003.
Hopley, D., 1986. Beachrock as a sea-level indicator. In: Van de Plassche, O. (Ed.), Sea-Level Research. Galliard Printers, Great Yarmouth, pp. 157–173.
Hori, K., Saito, Y., Zhang, Q., Wang, P., 2002. Architecture and evolution of the tide-dominated Changjiang (Yangtze) River delta, China. Sedimentary Geology 146, 249–264. https://doi.org/10.1016/S0037-0738(01)00122-1.
Howard, J.D., Frey, R.W., 1984. Characteristic trace fossils in nearshore to offshore sequences. Upper Cretaceous of east central Utah. Canadian Journal Earth Sciences 21, 200–219. https://doi.org/10.1139/e84-022.
Iturregui, A., Arrieta, N., Murelaga, X., Baceta, J.I., Olazabal, M.A., Martínez-Arkarazo, I., Madariaga, J.M., 2014. The relevance of the analytical methodology in the geochemical study of beachrock outcrops: Arrigunaga Beach inside the Nerbioi-Ibaizabal estuary (Getxo, Basque Country). Analytical Methods 6, 8247–8257. https://doi.org/10.1039/C4AY00913D.
Iturregui, A., Arrieta, N., Aramendia, J., Arrizabalaga, I., Murelaga, X., Baceta, J.I., Olazabal, M.A., Martínez-Arkarazo, I., Madariaga, J.M., 2016. In-situ and laboratory Raman spectroscopic analysis on beachrock deposits: characterisation of the trapped materials. Journal of Raman Spectroscopy 47, 329–336. https://doi.org/10.1002/jrs.4815.
Jennings, R., Shulmeister, J., 2002. A field based classification scheme for gravel beaches. Marine Geology 186, 211–228. https://doi.org/10.1016/S0025-3227(02)00314-6.
Kelly, C.S., Green, A.N., Cooper, J.A.G., Wiles, E., 2014. Beachrock facies variability and sea level implications: a preliminary study. In: Green, A.N., Cooper, J.A.G. (Eds.), Proceedings 13th International Coastal Symposium (Durban, South Africa). Journal of Coastal Research, Special Issue No. 70, pp. 736–742 https://doi.org/10.2112/SI70-124.1.
Khadkikar, A.S., Rajshekkar, C., 2003. Microbial cements in Holocene beachrocks of South Andaman Islands, Bay of Bengal. Current Science 84, 933–936.
Kleinhans, M.G., 2001. The key role of fluvial dunes in transport and deposition of sand–gravel mixtures, a preliminary note. Sedimentary Geology 143, 7–13. https://doi.org/10.1016/S0037-0738(01)00109-9.
Kleinhans, M.G., 2004. Sorting in grain flows at the lee side of dunes. Earth-Science Reviews 65, 75–102. https://doi.org/10.1016/S0012-8252(03)00081-3.
Knox, G.J., 1973. An aragonite-cemented volcanic beach-rock near Bilbao, Spain. Geologie en Mijnbown 53, 9–12.
Komar, P.D., Holman, R.A., 1986. Coast al processes and the development of shoreline erosion. Annual Review Earth Planetary Sciences 14, 237–265. https://doi.org/10.1146/annurev.ea.14.050186.001321.
Konhauser, K., 2007. Introduction to Geomicrobiology. Blackwell Publishing, Malden, MA, USA (425 pp.).
Krumbein, W.E., 1979. Photolithotropic and chemoorganotrophic activity of bacteria and algae as related to beachrock formation and degradation (Gulf of Aqaba, Sinai). Geomicrobiology Journal 1, 139–203. https://doi.org/10.1080/01490457909377729.
Martínez García, B., Pascual, A., Baceta, J.I., Murelaga, X., 2013. Estudio de los foraminíferos bentónicos del "beach-rock" de Azkorri (Getxo, Bizkaia). Geogaceta 53, 29–32.
Mauz, B., Vacchi, M., Green, A., Hoffmann, G., Cooper, A., 2015. Beachrock: a tool for reconstructing relative sea level in the far-field. Marine Geology 362, 1–16. https://doi.org/10.1016/j.margeo.2015.01.009.
McKee, E.D., 1957. Primary structures in some recent sediments. American Association Petroleum Geologist Bulletin 41 (8), 1704–1747. https://doi.org/10.1306/0BDA592D-16BD-11D7-8645000102C1865D.
Moore, C.H., 1973. Intertidal carbonate cementation in Grand Cayman, West Indies. Journal of Sedimentary Petrology 43, 591–602. https://doi.org/10.1306/74D72810-2B21-11D7-8648000102C1865D.
Moore, C.H., Billings, G.K., 1971. In: Bricker, O.P. (Ed.), Preliminary model of beachrock cementation, Grand Cayman island, B.W.I. Johns Hopkins Press, Baltimore, MD, pp. 40–43.
Neumeier, U., 1998. Le rôle de l'activité microbienne dans la cimentation précoce des beachrocks (sédiments intertidaux). (Ph.D. thesis)Terre et Environnement13. University of Geneva (183 pp.).
Neumeier, U., 1999. Experimental modelling of beachrock cementation under microbial influence. Sedimentary Geology 126, 35–46. https://doi.org/10.1016/S0037-0738(99)00030-5.
Passalia, M.G., Llorens, M., Césari, S.N., Limarino, C.O., Perez Loinaze, V.S., Vera, E.I., 2016. Revised stratigraphic framework of the Cretaceous in the Bajo Grande area (Argentinean Patagonia) inferred from new U–Pb ages and palynology. Cretaceous Research 60, 152–166. https://doi.org/10.1016/j.cretres.2015.11.004.
Pemberton, S.G., MacEachern, J.A., Dashtgard, S.E., Bann, K.L., Gingras, M.K., Zonneveld, J.-P., 2012. Shorefaces. Developments in Sedimentology. 64. Elsevier B.V., pp. 563–603. https://doi.org/10.1016/B978-0-444-53813-0.00019-8.
Pujalte, V., Astibia, H., Aizpiri, F., Payros, A., 2015. Las playas cementadas del "Antropoceno" de Bizkaia, País Vasco: origen y degradación. Geogaceta 57, 123–126.
Reesink, A.J.H., Bridge, J.S., 2007. Influence of superimposed bedforms and flow unsteadiness on formation of cross strata in dunes and unit bars. Sedimentary Geology 202, 281–296. https://doi.org/10.1016/j.sedgeo.2007.02.005.
Reesink, A.J.H., Bridge, J.S., 2009. Influence of bedform superimposition and flow unsteadiness on the formation of cross strata in dunes and unit bars – part 2, further experiments. Sedimentary Geology 222, 274–300. https://doi.org/10.1016/j.sedgeo.2009.09.014.
Reinson, G.E., 1984. Barrier-island and associated strand-plain systems. In: Walker, R.G. (Ed.), Facies ModelsGeoscience Canada, Reprint Seriesvol. 1. Geological Association Canada St. John's, pp. 119–140.
Rey, D., Rubio, B., Bernabeu, A.M., Vilas, F., 2004. Formation, exposure, and evolution of a high-latitude beachrock in the intertidal zone of the Corrubedo complex (Ria de Arousa, Galicia, NW Spain). Sedimentary Geology 169 (1–2), 93–105. https://doi.org/10.1016/j.sedgeo.2004.05.001.
Rodríguez-Navarro, C., Rodríguez-Gallego, M., Chekroun, K.B., Gonzalez-Muñoz, M.T., 2003. Conservation of ornamental stone by *Myxococcus xanthus*-induced carbonate biomineralisation. Applied Environmental Microbiology 69, 2182–2193. https://doi.org/10.1128/AEM.69.4.2182-2193.2003.

Rodríguez-Navarro, C., Jiménez-López, C., Rodríguez-Navarro, A., González-Muñoz, M.T., Rodríguez-Gallego, M., 2007. Bacterially mediated mineralization of vaterite. Geochimica et Cosmochimica Acta 71, 1197–1213. https://doi.org/10.1016/j.gca.2006.11.031.

Roep, T.B., Dabrio, C.J., Fortuin, A.R., y Polo, M.D., 1998. Late highstand patterns of shifting and stepping coastal barriers and washover-fans (Late-Messinian, Sorbas Basin, SE Spain). Sedimentary Geology 116, 27–56. https://doi.org/10.1016/S0037-0738(97)00111-5.

Sánchez-Moral, S., Cañaveras, J.C., Laiz, L., Saíz-Jiménez, C., Bedoya, J., Luque, L., 2003. Biomediated precipitation of calcium carbonate metastable phases in hypogean environments: a short review. Geomicrobiology Journal 20, 491–500. https://doi.org/10.1080/713851131.

Schmalz, R.F., 1971. Formation of beachrock at Eniwetok Atoll. In: Bricker, O.P. (Ed.), Carbonate Cements. Johns Hopkins Press, Baltimore, pp. 17–24.

Sherman, D.J., Bauer, B.O., 1993. Dynamics of beach-dune systems. Progress in Physical Geography 17, 413–447. https://doi.org/10.1177/030913339301700402.

Switzer, A.D., Jones, B.G., 2008. Setup, deposition, and sedimentary characteristics of two storm overwash deposits, Abrahams Bosom Beach, Southeastern Australia. Journal of Coastal Research 24, 189–200. https://doi.org/10.2112/05-0487.1.

Taylor, J.C.M., Illing, L.V., 1969. Holocene intertidal calcium carbonate cementation, Qatar, Persian Gulf. Sedimentology 12, 69–107. https://doi.org/10.1111/j.1365-3091.1969.tb00165.x.

Todd, S.P., 1989. Stream-driven, high-density gravelly traction carpets: possible deposits in the Trabeg Conglomerate Formation, SW Ireland, and some theoretical considerations of their origin. Sedimentology 36, 513–530. https://doi.org/10.1111/j.1365-3091.1989.tb02083.x.

Turner, R.J., 2005. Beachrock. In: Schwartz, M.L. (Ed.), Encyclopedia of Coastal Science. Kluwer Academic Publishers, The Netherlands, pp. 183–186.

Vousdoukas, M.I., Velegrakis, A.F., Plomaritis, T.A., 2007. Beachrock occurrence, characteristics, formation mechanisms and impacts. Earth-Science Reviews 85, 23–46. https://doi.org/10.1016/j.earscirev.2007.07.002.

Webb, G.E., Jell, J.S., Baker, J.C., 1999. Cryptic intertidal microbialites in beachrock, Heron Island, Great Barrier Reef: implications for the origin of microcrystalline beachrock cement. Sedimentary Geology 126 (1–4), 317–334. https://doi.org/10.1016/S0037-0738(99)00047-0.

Wiles, E., Green, A.N., Cooper, J.A.G., 2018. Rapid cementation on a South African beach: linking morphodynamics and cement style. Sedimentary Geology 378, 13–18. https://doi.org/10.1016/j.sedgeo.2018.10.004.

Zalasiewicz, J., Williams, M., Waters, C.N., Barnosky, A.D., Haff, P., 2014. The technofossil record of humans. The Anthropocene Review 1 (1), 34–43. https://doi.org/10.1177/2053019613514953.

Zammit, G., Sánchez-Moral, S., Albertano, P., 2011. Bacterially mediated mineralisation processes lead to biodeterioration of artworks in Maltese catacombs. Science of the Total Environment 409, 2773–2782. https://doi.org/10.1016/j.scitotenv.2011.03.008.